

Journal of Visualized Experiments

Assessing cell viability and death in 3D spheroid cultures of cancer cells

--Manuscript Draft--

Article Type:	Methods Article - JoVE Produced Video
Manuscript Number:	JoVE59714R1
Full Title:	Assessing cell viability and death in 3D spheroid cultures of cancer cells
Keywords:	Spheroids; 3D cell culture; hanging drop; cell viability; Breast cancer; pancreatic cancer; anti-cancer therapy; drug treatment; Chemotherapy; reconstituted basement membrane; propidium iodide; immunohistochemistry
Corresponding Author:	Stine Pedersen Kobenhavns Universitet Copenhagen, N/A DENMARK
Corresponding Author's Institution:	Kobenhavns Universitet
Corresponding Author E-Mail:	sfpedersen@bio.ku.dk
Order of Authors:	Michala G. Rolver Line O. Elingaard-Larsen Stine Pedersen
Additional Information:	
Question	Response
Please indicate whether this article will be Standard Access or Open Access.	Standard Access (US\$2,400)
Please indicate the city, state/province, and country where this article will be filmed . Please do not use abbreviations.	Copenhagen, Denmark

TITLE:

Assessing Cell Viability and Death in 3D Spheroid Cultures of Cancer Cells

AUTHORS AND AFFILIATIONS:

Michala G. Rolver, Line O. Elingaard-Larsen, Stine F. Pedersen

Section for Cell Biology and Physiology, Department of Biology, Faculty of Science,
University of Copenhagen, Copenhagen, Denmark

Email Addresses of Co-Authors:

Michala G. Rolver (cmh160@alumni.ku.dk)

Line O. Elingaard-Larsen (jbg748@alumni.ku.dk)

Corresponding Author:

Stine F. Pedersen (sfpedersen@bio.ku.dk)

KEYWORDS:

Spheroids, 3D cell culture, hanging drop, cell viability, breast cancer, pancreatic cancer, anti-cancer therapy, drug treatment, chemotherapy, reconstituted basement membrane, propidium iodide, immunohistochemistry

SUMMARY:

Here, we present several simple methods for evaluating viability and death in 3D cancer cell spheroids, which mimic the physico-chemical gradients of in vivo tumors much better than the 2D culture. The spheroid model, therefore, allows evaluation of the cancer drug efficacy with improved translation to in vivo conditions.

ABSTRACT:

Three-dimensional spheroids of cancer cells are important tools for both cancer drug screens and for gaining mechanistic insight into cancer cell biology. The power of this preparation lies in its ability to mimic many aspects of the in vivo conditions of tumors while being fast, cheap, and versatile enough to allow relatively high-throughput screening. The spheroid culture conditions can recapitulate the physico-chemical gradients in a tumor, including the increasing extracellular acidity, increased lactate, and decreasing glucose and oxygen availability, from the spheroid periphery to its core. Also, the mechanical properties and cell-cell interactions of in vivo tumors are in part mimicked by this model. The specific properties and consequently the optimal growth conditions, of 3D spheroids, differ widely between different types of cancer cells. Furthermore, the assessment of cell viability and death in 3D spheroids requires methods that differ in part from those employed for 2D cultures. Here we describe several protocols for preparing 3D spheroids of cancer cells, and for using such cultures to assess cell viability and death in the context of evaluating the efficacy of anticancer drugs.

INTRODUCTION:

The use of multicellular spheroid models in cancer biology is several decades old^{1,2}, but has gained substantial momentum in recent years. In large part, this reflects increased awareness of how strongly the phenotype of cancer cells is dependent on their

microenvironment and specific growth conditions. The microenvironment in solid tumors is fundamentally different from that in corresponding normal tissues. This includes physico-chemical conditions such as pH, oxygen tension, as well as interstitial pressure, concentration gradients of soluble factors such as nutrients, waste products, and secreted signaling compounds (growth factors, cytokines). Furthermore, it includes the organization of the extracellular matrix (ECM), cell-cell interactions and intercellular signaling, and other aspects of the particular three-dimensional (3D) architecture of the tumor³⁻⁶. The specific microenvironmental conditions in which cancer cells exist, profoundly affect their gene expression profile and functional properties, and it is clear that, compared to that of cells grown in 2D, the phenotype of 3D spheroids much more closely mimics that of in vivo tumors⁷⁻¹¹. 2D models, even if they employ hypoxia, acidic pH, and high lactate concentrations to mimic known aspects of the tumor microenvironment, still fail to capture the gradients of physico-chemical parameters arising within tumors, as well as their 3D tumor architecture. On the other hand, animal models are costly, slow, and ethically problematic, and generally, also have shortcomings in their ability to recapitulate human tumor conditions. Consequently, 3D spheroids have been applied as an intermediate complexity model in studies of a wide range of properties of most solid cancers^{9,11-17}.

A widely employed use of 3D spheroids is in screening assays of anticancer therapy efficacy^{9,18-20}. Treatment responses are particularly sensitive to the tumor microenvironment, reflecting both the impact of the tortuosity, restricted diffusion, high interstitial pressure, and acidic environmental pH on drug delivery, and the impact of hypoxia and other aspects of the microenvironment on the cell death response^{9,17}. Because the environment within 3D spheroids inherently develops all of these properties⁷⁻¹¹, employing 3D cell cultures can substantially improve the translation of results to in vivo conditions, yet allow efficient and affordable high-throughput screening of the net growth. However, the great majority of studies on the drug response of cancer cells are still carried out under 2D conditions. This likely reflects that, while some assays can relatively easily be implemented for 3D cell cultures, many, such as viability assays, western blotting, and immunofluorescence analysis, are much more conveniently done in 2D than in 3D.

The aim of the present work is to provide easily amenable assays and precise protocols for analyses of the effect of treatment with anti-cancer drugs on cancer cell viability and survival in a 3D tumor mimicking setting. Specifically, we provide and compare three different methods for spheroid formation, followed by methods for qualitative and quantitative analyses of growth, viability and drug response.

PROTOCOL

1. Generation of spheroids

1.1. Preparing cell suspensions for spheroid formation

NOTE: Different cell lines have very different adhesion properties and the most suitable spheroid formation protocol must be established in each case. It was tested that MCF-7 and BxPC-3 cells are suitable for spontaneous spheroid formation, while MDA-MB-231, SKBr-3, Panc-1 and MiaPaCa require the addition of reconstituted basement membrane to

successfully form spheroids. Only MDA-MB-231 and BxPC-3 cells have been employed for the hanging drop protocol, however other cell lines are certainly applicable.

1.1.1. Grow cells as monolayer until 70-80% confluency.

1.1.2. Wash cells with phosphate buffered saline (1x PBS, 5 mL for a 25 cm² or 10 mL for a 75 cm² flask), add the cell dissociation enzyme (0.5 mL for a 25 cm² or 1 mL for a 75 cm² flask) and incubate the cells for 2-5 min at 37 °C in 5% CO₂ and 95% humidity.

1.1.3. Check the cell detachment under a microscope and neutralize the cell dissociation enzyme by adding growth medium (6-10% serum depending on the cell line) to a total volume of 5 mL in a 25 cm² or 10 mL for a 75 cm² flask.

1.1.4. Use a Bürker chamber to count cells (**Figure 1A (i)**) and count 8 squares in the chamber per cell preparation to obtain a high reproducibility of the size of the spheroids.

NOTE: Three protocols each describing a different method for spheroid formation are presented below. Protocol 1.2 and 1.3 can be used for all the subsequent analytic protocols presented, whereas protocol 1.4 is best suited for embedding and lysate preparations. Depending on the cell line, spheroid formation takes 2-4 days, irrespective of the method used.

1.2. Spontaneous spheroid formation

1.2.1. Perform steps 1.1.1-1.1.4.

1.2.2. Dilute the cell suspension in a 15 mL tube to obtain 0.5-2 x 10⁴ cells/mL (optimal cell density needs to be determined for each cell line) (**Figure 1A (ii)**).

1.2.3. Transfer the cell suspension to a sterile reservoir and, using a multichannel pipette, dispense 200 µL/well into ultra-low attachment 96-well round bottom plates (**Figure 1A (iii)**). Fill the outer ring of wells with 1x PBS or growth medium to reduce evaporation from the remaining wells.

1.2.4. Incubate the plate in an incubator at 37 °C with 5% CO₂, 95% humidity.

1.2.5. Every 2-3 days acquire light microscopic images of the spheroids.

NOTE: The images in this paper are taken at 11.5x magnification, which is appropriate for most spheroids prepared using these protocols.

1.2.6. Every 2-3 days (after acquiring images) replace 100 µL of medium (remove 100 µL of the spent medium and replace with 100 µL of fresh medium).

NOTE: To avoid removing spheroids when replacing medium, it is advisable to tilt the plate a bit while slowly removing the medium and inspect the aspirated medium in the tips for

visible spheroids before discarding it.

1.3. Reconstituted basement membrane-mediated spheroid formation.

NOTE: Lactose dehydrogenase elevating virus (LDEV)-free reduced growth factor reconstituted basement membrane (rBM) was used. rBM is temperature-sensitive and should always be kept on the ice, as it will clot if it reaches 15 °C. Thaw the rBM on ice either overnight at 4 °C or 2-4 h at room temperature (RT) before plating.

1.3.1. Thaw rBM on ice (see **Table of Materials**).

1.3.2. Keep plates and reservoirs (if individually wrapped) on the ice before use.

1.3.3. Perform steps 1.1.1-1.1.4.

1.3.4. Dilute the cell suspension in a 15 mL tube to obtain $0.5-2 \times 10^4$ cells/mL (optimal cell density needs to be determined for each cell line) (**Figure 1A (ii)**).

1.3.5. Place the 15 mL tube containing the diluted cell suspension on the ice (e.g., in glass beaker) (**Figure 1A (iia)**).

1.3.6. Transfer the chilled plates and reservoirs to the hood. Rinse plastic containers, fill them with ice and transfer them into the hood to allow the plates and reservoirs to be placed on ice during the entire procedure.

1.3.7. Resuspend rBM gently to ensure a homogenous gel.

1.3.8. Add 1-2% rBM (optimal concentration needs to be determined for each cell line) to the chilled cell suspensions (**Figure 1A (iib)**).

1.3.9. Invert the 15 mL tube to ensure the proper mixing of rBM and cell suspension before dispensing the suspension into the plate.

1.3.10. Transfer the rBM-containing cell suspension to a sterile reservoir and dispense 200 μ L/well into chilled ultra-low attachment 96-well plates using a multichannel pipette (**Figure 1A (iii)**).

NOTE: If working with several cell suspensions (e.g., more than one cell line), it is essential to dispense each cell suspension immediately after rBM addition to prevent premature gelling.

1.3.11. Centrifuge the plate for 15 min at 750 x g (if possible, at 4 °C to keep the rBM fluid longer but not a requirement for successful spheroid formation), to ensure that the cells are clustered together when the rBM hardens, facilitating the formation of one single spheroid.

1.3.12. Incubate the plate in an incubator (37 °C, 5% CO₂, 95% humidity).

1.3.13. Every 2-3 days acquire light microscopic images for evaluation of spheroid growth.

1.3.14. Every 2-3 days replace 100 μ L of medium (remove 100 μ L and replace with 100 μ L of fresh medium).

1.4. Hanging drop spheroids.

1.4.1. Perform step 1.1.1-1.1.4.

1.4.2. Dilute cells to obtain a suitable dilution. A practical dilution is 50,000 cells/mL.

1.4.3. Remove the lid of a 10 cm² cell culture dish and place it so it faces upwards. Add 6 mL of 1x PBS to the dish (**Figure 1B (i)**).

1.4.4. Pour the cell suspension into a sterile reservoir and carefully place up to 30 drops of 40 μ L of cell suspension onto the lid of the cell culture dish using a multichannel pipette (**Figure 1B (ii)**), resulting in a concentration of 2,000 cells/drop. Avoid placing the drops too close to the edge of the lid as these drops are more likely to lose surface tension when inverting the lid in the following step.

1.4.5. Invert the lid in a quick but controlled movement and place it on top of the 1x PBS-containing cell culture dish (**Figure 1B (iii)**).

1.4.6. Place the dish in an incubator at 37 °C with 5% CO₂ and 95% humidity without disturbing the drops and leave them to grow for 4-6 days.

1.4.7. If to be used for protein lysates or embedding, pool spheroids by removing the lid and tilt it, in order to wash down the drops with 1 mL of heated media. Transfer the resulting media containing spheroids to a 1.5 mL tube and allow them to settle to the bottom of the tube. Proceed as described in 5.4 and 6.2.2 for protein lysates and embedding, respectively.

2. Drug treatment of spheroids

NOTE: Long-term drug treatment can be applied to the spheroids in order to screen for effects of a drug of interest. Before initiating the drug treatment, it is advisable to perform a dose response experiment of the drug(s), in order to find an appropriate dose for the experimental treatment. The doses should be based on the determined IC₅₀/K_i of the drug and range from around 0.2x-10x of this value.

2.1. Set up 6-12 spheroids per the desired condition as described in 1.2 or 1.3 and place in the incubator (37 °C, 5% CO₂, 95% humidity) for 2 days.

2.2. On day 2, take light microscopic images of the spheroids.

2.3. Prepare the first treatment doses (after acquiring images).

NOTE: The first treatment concentration must be twice the desired final concentration as the solution will be diluted 1:2 upon addition to the well containing 100 μ L medium. Suggested drug treatment intervals (will depend on drug half-life): Day 2, 4 and 7.

2.4. Using a multichannel pipette, gently remove 100 μ L of medium and replace it with 100 μ L of drug containing medium.

2.5. Place the 96-well plate back in the incubator at 37 °C with 5% CO₂ and 95% humidity and repeat 2.3 and 2.4 on the chosen days of treatment but now without doubling the dose to obtain correct final dose.

2.6. On the final day of the protocol/treatment schedule, one or several of the following assays can be performed.

3. Cell viability assay for spheroids

3.1. Set up 4-6 spheroids per the desired condition as described in 1.2 or 1.3 and place in the incubator at 37 °C with 5% CO₂ and 95% humidity.

NOTE: In this case, the cell viability assay was performed on day 7 or 9, after having monitored spheroid growth every 2-3 days by light microscopy as described above (point 1.2.5 and 1.3.13).

3.2. Thaw the viability assay reagent (see **Table of Materials**) and let it equilibrate to RT prior to use.

3.3. Mix gently by inverting to obtain a homogeneous solution.

3.4. Before performing the assay, remove 50% of the culture medium from the spheroids (100 μ L).

3.5. Add cell viability reagent to each well at a 1:3 ratio to the amount of medium present in the well (**Figure 2A (i)**) For a 96-well plate, add 50 μ L of reagent to 100 μ L of medium.

3.6. Mix the contents vigorously for 5 min to induce cell lysis (**Figure 2A (ii)**).

3.7. Incubate for 25 min at RT to stabilize the luminescent signal (**Figure 2A (iii)**).

3.8. Record the luminescent signal (**Figure 2A (iv)**).

4. Propidium iodide (PI) staining of spheroids

4.1. Set up 3-6 spheroids per desired the condition as described in 1.2 or 1.3 and place in the incubator at 37 °C with 5% CO₂ and 95% humidity.

4.2. In a sterile cell culture lab, heat 1x PBS to 37 °C.

4.3. Make a PI solution of 4 μ M by diluting stock solution in 1x PBS: Dilute a 1 mg/mL aqueous stock of PI 1:350 in 1x PBS.

NOTE: This concentration will be further halved upon addition of the solution to the wells giving a final concentration of 2 μ M. 100 μ L of this solution is needed for each well containing a spheroid.

CAUTION: Propidium iodide (PI) must be handled in a fume hood and wearing gloves. PI is light sensitive. Protect from light when handling.

4.4. Remove 100 μ L of the medium from each well in the 96-well plate without removing the spheroids.

4.5. Wash out the remaining medium by adding 100 μ L of heated 1x PBS to all wells followed by removing 100 μ L of the liquid in the wells. Repeat this washing step 3 times.

4.6. Add 100 μ L of the PI solution to each well, cover the plate in aluminum foil and place it in an incubator at 37 $^{\circ}$ C with 5% CO₂ and 95% humidity for 10-15 min.

4.7. Repeat the 3 washing steps described in 4.5 to wash out PI solution, in order to diminish background signal when imaging.

4.8. Use an epifluorescence microscope to image the spheroids. To evaluate the viability of cells in the spheroid core take z-stacks to get images with varying depths of the spheroid.

NOTE: A step size around 18-35 μ m between each slice depending on spheroid size is advisable, giving approximately 11-18 stacks per spheroid. Z-stacks can be processed in ImageJ using the z-projection function, which can combine all z-stacks into one final picture, giving an overview of the staining throughout the spheroid (for further guidelines on the use of ImageJ for this purpose, see (<https://imagej.net/Z-functions>)).

5. Preparing protein lysates for western blotting from 3D spheroid cultures

NOTE: When collecting the spheroids, it is advisable to use a P200 pipette and cut the end of the tip to allow a bigger opening and hence an easier capture of the spheroids without disturbing their structure.

5.1. For each condition, pool a minimum of 12, ideally 18-24 spheroids (depending on spheroid size) in a 1.5 mL tube (avoid 2 mL tubes, as the next steps will become more difficult due to their less pointy bottom).

NOTE: If the amount of medium exceeds 1.5 mL before having collected all the spheroids, allow the collected spheroids to settle at the bottom (happens very quickly, centrifugation not necessary) and discard half the volume of the tube before continuing collecting the remaining spheroids.

5.2. Place tubes on ice and allow the spheroids to settle at the bottom of the 1.5 mL tube.

5.3. Move from the sterile cell laboratory to the regular laboratory.

5.4. Wash spheroids twice in 1 mL of ice-cold 1x PBS. Let spheroids settle before removing 1x PBS between each washing step.

5.5. Aspirate as much 1x PBS as possible without disturbing or removing the spheroids.

5.6. Add 5 μ L of heated lysis buffer (LB) with phosphatase- and protease inhibitors, per spheroid (e.g., 10 spheroids = 50 μ L LB).

5.7. Repeat intervals of vortex followed by spin down until spheroids are dissolved. Perform a cycle of vortexing for 30 s followed by centrifugation (a quick spin using a tabletop centrifuge is sufficient) for 10 s for approx. 5-10 min depending on the size and the compactness of the spheroids.

NOTE: The protocol can be paused here. Keep the lysates at -20 °C until proceeding with sonication, homogenization and protein determination as in a standard 2D protein lysate protocol, followed by western blotting using standard protocols.

6. Embedding of 3D spheroids

6.1. Prepare the agarose gel into which the spheroids are embedded (only necessary first time performing the protocol).

6.1.1. Mix 1 g of bactoagar in 50 mL of ddH₂O.

6.1.2. Heat slowly in microwave oven until the bactoagar has dissolved and a homogenous gel has formed. Do not allow the gel to boil.

6.1.3. Keep it warm in a water bath at 60 °C.

6.1.4. Keep at 4 °C between experiments.

6.2. Embedding of spheroids.

6.2.1. On day 1, for each condition, pool a minimum of 12 spheroids in a 1.5 mL tube.

6.2.2. Wash once with 1 mL of ice-cold 1x PBS.

6.2.3. To fix the spheroids, add 1 mL of 4% paraformaldehyde.

6.2.4. Let them incubate for 24 h at RT.

6.2.5. On day 2, heat the agarose gel carefully by placing it in a water-filled beaker in a microwave oven. Ensure that the gel does not boil! Keep warm in a benchtop heating plate,

at 60 °C until use.

6.2.6. Wash spheroids twice with 1 mL of ice-cold 1x PBS.

6.2.7. Aspirate most of the 1x PBS (leaving approximately 100 µL at this point is practical for handling the spheroids).

6.2.8. Prepare a 20 µL pipette by cutting the pipette tip at an incline to obtain a pointier tip with a larger hole (see illustration).

NOTE: The next part has to be done quickly to ensure optimal spheroid transfer and to avoid solidification of gel drop. If no heating block is available, it is recommended to first catch the spheroids and then make the agarose drop (i.e., switching the order of points 6.2.9 and 6.2.10).

6.2.9. Make an agarose gel drop on a microscope slide. Place the slide on a warm heating block to prevent the agarose from solidifying.

6.2.10. Using the modified pipette tip (see 6.2.8), catch as many spheroids as possible in a volume of 15-20 µL.

6.2.11. Carefully inject the 15-20 µL spheroid-containing 1x PBS into the center of the agarose gel drop without touching the microscope slide.

NOTE: This is a slightly difficult point. The spheroids will be lost if the pipette tip touches the microscope slide when injecting the spheroids into the gel drop. It is advisable to practice the whole process of making the agarose drop and injecting the spheroids by injecting a colored liquid into the drop. This will allow visualization of a potential penetration through the drop, as the colored liquid will be leaking out onto the slide.

6.2.12. Let the agarose gel drop harden by incubating for 5-10 min at RT or at 4 °C. Once the gel drop has solidified somewhat (but still rather soft), carefully push the gel drop from the microscope slide into a plastic tissue cassette with a scalpel.

6.2.13. Cover the plastic tissue cassettes in 70% ethanol.

NOTE: At this point the spheroids can be used directly or stored for months.

6.2.14. Embed the agarose-embedded spheroid in paraffin, section into 2-3 µm thick layer slides and stain with hematoxylin and eosin or subject to immuno-histological staining.

REPRESENTATIVE RESULTS

Spheroid growth assays based on the spheroid formation protocol schematically illustrated in **Figure 1A** and **Figure 1B**, were used as a starting point for analysis of the effects of anti-cancer drug treatments in a 3D tumor mimicking setting. The ease with which spheroids are formed is cell line specific, and some cell lines require supplementation with rBM in order to form coherent spheroids²². The concentration of rBM added can profoundly affect the

morphology of the spheroids. As shown in **Figure 1C** and **Figure 1D**, varying the concentration of rBM between 0 and 4% alters the compactness and morphology of the spheroids in a cell type dependent manner. **Figure 1C** demonstrates how the addition of up to 2.5% rBM allows spheroid formation in SKBr-3 breast cancer cells, with no further effect at concentrations above 2.5% rBM. In contrast, BxPC3 pancreatic ductal adenocarcinoma (PDAC) cells, which exhibit an epithelial morphology, spontaneously form small, compact spheroids (**Figure 1D**, upper, left panel). In this cell type, increasing rBM concentration to 1.5% or above elicits a distinct morphological change from spheroid to more convoluted structures with protrusions and invaginations, reminiscent of ductal tubular structure formation. Conversely, the addition of rBM to two other PDAC cell lines, MiaPaCa and Panc-1, which have a more mesenchymal phenotype, allows the loose cellular aggregates to become tighter and form more compact spheroids (**Figure 1D**, middle and lower panels). These results show that the precise amount of rBM resulting in optimal spheroid formation must be titrated for each cell line and condition.

A quantitative assessment of cell viability within the spheroids upon drug treatment was necessary to evaluate the effect of anti-cancer drug treatments. The assay described here is a luciferin-luciferase-based assay, which measures ATP released from live cells within spheroids. The principle of the assay is illustrated in **Figure 2A**. The luminescent signal generated in this assay is easily recorded by a plate reader (**Figure 2A**) and correlates well with viability measured by other methods²³. The linear relation between ATP concentration and luminescence in the relevant concentration range is shown in **Figure 2B**, while **Figure 2C** shows the ability of the assay to assess cell death in 3D spheroids treated with anti-cancer therapy. In order to further evaluate the linearity of the assay in the relevant range, experiments to establish standard curves of the luminescent signal as a function of the number of cells were carried out (**Figure 2D** and **Figure 2E**). These results indicate that the assay is suitable for estimating cell viability in 3D spheroid cultures and that it is applicable for investigating drug-induced loss of cell viability.

A combination of light microscopic images acquired every two to three days, during the treatment period and a final quantitative assessment of cell viability allows close supervision of spheroid growth and morphology as well as the assessment of optimal treatment dose. The latter is exemplified in **Figure 3A** and **Figure 3B**, where a dose-response experiment was performed to determine the dose necessary for 50% reduced cell viability in MDA-MB-231 breast cancer spheroids. Treatment effects on spheroid morphology are visualized in **Figure 3C** and **Figure 3D** for MDA-MB-231 and MCF-7 spheroids, respectively. During treatment with the chosen chemotherapeutic cocktail, the compactness of MDA-MB-231 spheroids increases, while during treatment with tamoxifen, MCF-7 spheroids become increasingly frayed and uneven. In both cases, a clear drop in cell viability is visible after 7 (MDA-MB-231) or 9 (MCF-7) days of treatment (**Figure 3E** and **Figure 3F**). This demonstrates the need for both a visual and a quantitative assessment of treatment-mediated effects on spheroid cell viability and morphology as well as that these parameters are highly cell- and treatment-type specific.

As a supplement to the cell viability assay, staining of dead cells with PI, which cannot cross the membrane and therefore only stains necrotic or late apoptotic cells with compromised membrane integrity, allows for a quick spatial evaluation of dead cells in response to

treatment, without the time-consuming protocol of embedding, sectioning and IHC. As illustrated in **Figure 4A** the spatial arrangement of dead cells upon an increasing concentration of an inhibitor, in this case, the Na⁺/H⁺ exchanger 1 (NHE1) inhibitor 5-(N-ethyl-N-isopropyl)-amiloride (EIPA), can be visualized. As seen, control and vehicle spheroids show a limited necrotic/late apoptotic core, whereas the dead cells are distributed throughout the spheroid as the concentration of EIPA is increased.

In order to quantify the relative induction of apoptotic stress following different treatments, spheroids were lysed and subjected to SDS-PAGE gel electrophoresis and western blotting for full-length and cleaved poly (ADP-ribose) polymerase (PARP). Representative results are shown in **Figure 4B** and **Figure 4C**. In this experiment, spheroids were prepared from MDA-MB-231 cells in which the lactate-proton cotransporter MCT4 or the Na⁺, HCO₃⁻ cotransporter NBCn1 were knocked down using siRNA. The knockdown was evaluated by western blotting for MCT4 and NBCn1 (unpublished data). As seen, the knockdown of MCT4, but not of NBCn1, robustly increases PARP cleavage, consistent with our previous demonstration that stable knockdown of MCT4 in MDA-MB-231 cells decreases tumor growth *in vivo*²⁴.

To further analyze the effects of treatment and obtain information on the specific signaling-, growth arrest, and death pathways activated, the spheroids can in addition to western blot analysis be embedded and subjected to immunohistochemistry (IHC) analysis. IHC analysis of the spheroid sections allows the use of specific antibodies or markers of cell proliferation, cell cycle and programmed cell death, and facilitates a visualization of the spatial arrangement of proliferative and apoptotic cells in the spheroid.

A schematic figure of the embedding protocol for IHC analysis of spheroids is presented in **Figure 5A**. A representative light microscopic image of an approx. 3 μm thick microtome section of an embedded spheroid is shown in **Figure 5B**, and an immunofluorescence image of a spheroid stained for the tumor suppressor protein p53 (nuclei stained using DAPI), is shown as **Figure 5C**. Examples of DMSO and chemotherapy-treated spheroids stained for the cell proliferation marker Ki-67 or for p53 are shown in **Figure 5D** and **Figure 5E**, respectively. Consistent with the antiproliferative effect of the chemotherapy treatment, the number of Ki-67 positive cells are greater in the DMSO control than in the chemotherapy-treated spheroid (**Figure 5D**). In contrast, p53 expression is increased during conditions of cell stress, apoptosis and growth arrest, and consequently, the number of p53-stained cells is substantially higher in the chemotherapy-treated spheroids compared to DMSO controls (**Figure 5E**).

These results illustrate examples of how spatially resolved (PI staining, IHC) or quantitative (western blotting) information on drug treatment effects in 3D spheroids can be obtained.

FIGURE LEGENDS:

Figure 1. Spontaneous and rBM-mediated spheroid formation. (A) Schematic representation of spheroid formation using ultra-low attachment 96-well round bottom plates, with optional use of rBM. Individual steps marked by (i-iii). (B) Schematic representation of spheroid formation using the hanging drop method. Individual steps are marked by (i-iii) (C) Representative images of rBM-mediated spheroid formation of SKBr-3

cells. Cells were seeded in ultra-low attachment 96-well round bottom plates with increasing concentrations of rBM and grown for 9 days. Scale bar: 100 μ m. n=3. (D) Representative images of BxPC-3, MiaPaCa and Panc-1 cells seeded for spheroid formation in ultra-low attachment 96-well round bottom plates with concentrations of rBM from 0.5-2.5 %. Spheroids were grown for 4 days. Scale bar: 250 μ m. n=3.

Figure 2. Principle and evaluation of the cell viability assay. (A) Schematic representation of the 3D cell viability assay. Individual steps denoted by (i-iv). (B) Luminescent signal as a function of ATP concentration. Dilutions of ATP were plated in a 96-well plate and cell viability reagent added to each well. Luminescence was recorded after 30 min at 405 nm. 1 n. (C) Viability, measured as luminescence, of control and chemotherapy-treated MCF-7 spheroids. MCF-7 cells were seeded in ultra-low attachment round-bottom plates and were grown for 7 days. Chemotherapy treatment (5 μ M Cisplatin, 5 μ M Doxorubicin and 30 nM 5-FU) was applied on day 2 and 4. Bars represent mean values with SD. 1 n. (D) Luminescent signal as function of the number of MCF-7 cells seeded. MCF-7 cells were seeded in 96-well plates at the indicated cell number and allowed to grow for 48 h, after which cell viability was measured. Error bars represent SD. 1 n. (E) As described in D for MDA-MB-231 cells.

Figure 3. Effects of treatment regimens on spheroid morphology and cell viability. (A) Representative images of MDA-MB-231 spheroids on day 2, 4 and 7. MDA-MB-231 cells were seeded in ultra-low attachment round bottom 96-well plates. Treatment with increasing doses of chemotherapy was started on day 2, at which time all spheroids were of similar size. Rows show spheroids at increasing doses of chemotherapy, and columns show spheroids representative of size at day 2, 4, and 7 at the indicated dose. The lowest dose was 18.75 nM Cisplatin, 18.75 nM Doxorubicin, 0.0625 nM 5-Fluorouracil (5-FU) and this dose was doubled for each image shown, resulting in a maximal dose of 0.3 μ M Cisplatin, 0.3 μ M Doxorubicin and 2 nM 5-FU. Scale bar: 100 μ m. 2 n. (B) Viability of MDA-MB-231 spheroids, measured as luminescence, after 7 days of chemotherapeutic treatment. The bars represent mean values with SEM. 2 n. (C,D) Representative images of MDA-MB-231 (C) and MCF-7 spheroids (D) on day 2, 4, 7 and for MCF-7 spheroids 9. Cells seeded as in (A) and treated with either chemotherapy (Chemo, 18.75 nM Cisplatin, 18.75 nM Doxorubicin, 0.0625 nM 5-FU) on day 2 and 4 (C) or with 2 μ M Tamoxifen (Tam) on day 2, 4 and 7 (D). Scale bar: 100 μ m. 4 n and 3 n, respectively. (E,F) Viability, measured as luminescence, on day 7 and 9 for (C) and (D), respectively. To test for statistically significant difference between conditions an unpaired Student's t-test was performed. **** denotes $p < 0.0001$.

Figure 4. Propidium iodide staining and western blot analysis of spheroids. (A) Representative images of PI-stained MCF-7 spheroids after 9 days of treatment. MCF-7 cells were seeded in ultra-low attachment 96-well plates grown for 9 days and treated with increasing concentrations of EIPA on day 2, 4 and 7. On day 9, the spheroids were stained with PI and images were acquired on an epifluorescence microscope. Scale bar: 200 μ m. 1 n. (B) Representative western blots of MDA-MB-231 cells after knockout/knockdown of acid-base transporters. NHE1 was knocked out by CRISPR/Cas9 in MDA-MB-231 cells¹² and the cells were subsequently transiently transfected with siRNA against MCT4 or NBCn1, and grown as spheroids for 9 days before being lysed and subjected to western blotting using an antibody recognizing total and cleaved (c)PARP. (C) Quantification of the ratio of cPARP to PARP protein level, normalized to loading control (β -actin). 1 n.

Figure 5. Fixing, embedding and immunohistochemistry analysis of spheroids. (A) Schematic representation of the protocol for embedding of spheroids. Individual steps are marked as (i-vii). (B) Image of embedded MDA-MB-231 spheroid. Scale bar: 50 μ m. (C) Representative image of chemotherapy-treated MDA-MB-231 spheroid subjected to IHC analysis with antibodies against p-53. Dashed lines show the circumference of the spheroid. Scale bar: 20 μ m. (D,E) Representative images of DMSO- or chemotherapy-treated (upper and lower panels, respectively) MDA-MB-231 spheroids. MDA-MB-231 cells were seeded in ultra-low attachment 96-well plates, grown for 7 days and treated with chemotherapy on day 2 and 4. On day 7, the spheroids were embedded followed by analysis by IHC with primary antibodies against Ki-67 (D) and p53 (E). White boxes represent zoom images. Scale bar: 20 μ m in both magnifications, n=3.

DISCUSSION

The use of 3D cancer cell spheroids has proven a valuable and versatile tool not only for anticancer drug screening, but also for gaining mechanistic insight into the regulation of cancer cell death and viability under conditions mimicking those in the tumor microenvironment. This is particularly crucial as the accessibility, cellular uptake, and intracellular effects of chemotherapeutic drugs are profoundly impacted by the physico-chemical conditions in the tumor, including pH, oxygen tension, tortuosity, and physical and chemical cell-cell interactions^{9,17}. For example, the acidity of extracellular pH, which can reach values as low as 6-6.5 in many solid tumors²⁵⁻²⁹, causes weakly basic chemotherapeutic compounds, such as doxorubicin, mitoxantrone and the zwitterion paclitaxel, to be charged. This reduces their uptake into the tumor cells and can influence the activity of multidrug resistance proteins such as p-glycoprotein³⁰⁻³². Also the cell proliferation, which is pivotal to the effect of most chemotherapeutic compounds, is generally reduced in 3D compared to 2D conditions and hence is likely better mimicked in tumor spheroids than in 2D cell culture^{8,33,34}. Finally, the dense tumor microenvironment is the origin of numerous physical and soluble signaling cues directing intracellular signaling pathways regulating cell growth, survival and death. Thus, when analyzing drug efficacy, 3D culture systems are a pivotal step before embarking on in vivo models. A major drawback of 3D culture is, however, the increased complexity of analysis compared to that of 2D culture. We have described here simple and relatively inexpensive techniques for spheroid formation using a variety of cancer cell types. We have shown examples of how spheroid formation must be optimized for each cell type studied and have described how to obtain quantitative data on cell viability, cell death, and associated signaling pathways, in such spheroids. There is no obvious growth- or morphological differences between the three models described here. In our hands, the variation in morphology may be slightly greater using the hanging drop method, yet an advantage of this method is that rBM is not needed. We have focused here on spheroids produced from a single cancer cell type. The spheroid model is, however, also amenable to co-culture, for instance of cancer cells with fibroblasts, monocytes/macrophages, endothelial cells, and/or adipocytes³⁵⁻³⁷. Other advanced applications of this model include the combination with 3D printed fluidic devices allowing dosing through a semipermeable membrane, followed by harvesting for quantitative proteomic profiling³⁸.

While, as noted above, the phenotype of cells grown in 3D spheroids generally mimics that of in vivo tumors much better than do cells grown in 2D, the extent to which such spheroids are in fact relevant models of the corresponding in vivo tumors is dependent on numerous factors and has to be carefully evaluated. Parameters which will impact how well such spheroids mimic the in vivo condition include the cellular composition of the tumor and its relative ECM composition. For instance, the rBM which we have employed as ECM in the protocols provided here is a good choice for mimicking early stages of epithelial cancers, around the time of breaching the basement membrane, other ECM compositions will be more relevant for certain tumor types and -stages. Furthermore, the capacity for cell-cell adhesion differs widely between cancer cell lines, depending on their expression of cell-cell and cell-matrix adhesion proteins such as cadherins and integrins²².

As described here, spheroid growth and morphology can easily and non-invasively be monitored every 2-3 days using a light microscope with low magnification optics and a large field of view. However, because the cytotoxic stress, such as chemotherapy treatment, affects spheroid morphology very differently and, in a manner, depending on the cell type and treatment scheme, it is not enough to rely on the morphology and circumference alone for evaluating treatment effect. For instance, spheroids may become looser with treatment and emerging cell death, or all death may occur in the necrotic core, while the surface is not detectably affected. In both cases, the result may be an erroneous impression that the number of live cells in the spheroid is not reduced by the treatment. Quantitative- and whole-spheroid techniques are therefore essential for evaluating treatment effect. For quantitative evaluation of cell death, the acid phosphatase assay, which as the name implies measures the activity of cytosolic acid phosphatase has been employed²¹. However, in our hands, while this assay generally nicely reflects the number of cells seeded, it does not adequately capture rapid treatment-induced cell death (data not shown), likely because the acid phosphatase remains active for some time after cell death. Furthermore, this assay requires complete removal of the medium, which increases error especially with fragile, chemotherapy-treated spheroids. The cell viability assay described here, which is based on cellular ATP content, was chosen based on its simple and time efficient protocol and high reproducibility. Furthermore, this assay does not require complete removal of culture medium which is an advantage when working with spheroids. As shown in representative results, this assay captures well both cell number and expected chemotherapy treatment effects. However, a pitfall of this technique is, obviously, that metabolic changes reducing intracellular ATP content may erroneously be recorded as a lower cell number. Hence, parallel assessment of spheroid volume and morphology, or PI staining, is advisable to validate results.

Spheroid lysis followed by western blotting can provide semi-quantitative insight into the state of signaling processes, cell death-, growth- and viability pathways. The use of western blotting is complicated when rBM is used to prepare the spheroids, since this will comprise a substantial fraction of the lysate protein content, and more importantly, its fractional contribution will increase with decreasing cellular content during chemotherapeutic cell death. It is in principle possible to remove the rBM by centrifugation; however, this is a critical step, as it is difficult to completely remove all rBM, and this will preclude quantitative comparison between conditions. For such spheroids, and in general for spatially resolved assessment of death pathways and relevant signaling parameters, embedding and

IHC are strong tools. Other approaches may be considered: live confocal imaging of (relatively small) intact spheroids³⁹. Another interesting property of spheroids is that given their rather regular “ball” shape, they lend themselves well to iteration between mathematical modeling and wet lab experiments, to increase the understanding of the importance of the above-mentioned gradients of oxygen, pH, and nutrients within spheroids, and, by extrapolation, tumors^{40,41}. Thus, although important 3D tumor models of much greater complexity are emerging, including a wide range of organotypic and organoid cultures based on complex biological as well as inert scaffolds, and, not least, patient-derived xenografts⁴², spheroids remain an important tool because of their superior biological relevance compared to 2D culture, combined with relative ease of handling.

In summary, we present here a series of simple methods for analysis of anti-cancer treatment-induced changes in cancer cell viability and death in 3D culture. The composition of the spheroids can be modified depending on the properties and biology of the cells employed, and the quantitative and qualitative analyses presented are useful both for assessing dose-response relationships and for gaining insight into the signaling- and death pathways involved.

ACKNOWLEDGMENTS

We are grateful to Katrine Franklin Mark and Annette Bartels for excellent technical assistance and to Asbjørn Nøhr-Nielsen for performing the experiments in Figure 1D. This work was funded by the Einar Willumsen Foundation, the Novo Nordisk Foundation, and Fondation Juchum (all to SFP).

DISCLOSURES

The authors declare no conflict of interest.

REFERENCES

- 1 Sutherland, R. M. Cell and environment interactions in tumor microregions: the multicell spheroid model. *Science*. **240** (4849), 177-184 (1988).
- 2 Mueller-Klieser, W., Freyer, J. P., Sutherland, R. M. Influence of glucose and oxygen supply conditions on the oxygenation of multicellular spheroids. *British Journal of Cancer*. **53** (3), 345-353 (1986).
- 3 Gaedtke, L., Thoenes, L., Culmsee, C., Mayer, B., Wagner, E. Proteomic analysis reveals differences in protein expression in spheroid versus monolayer cultures of low-passage colon carcinoma cells. *Journal of Proteome Research*. **6** (11), 4111-4118 (2007).
- 4 Chen, J. L. et al. The genomic analysis of lactic acidosis and acidosis response in human cancers. *PLoS Genetics*. **4** (12), e1000293 (2008).
- 5 Cukierman, E., Pankov, R., Stevens, D. R., Yamada, K. M. Taking cell-matrix adhesions to the third dimension. *Science*. **294** (5547), 1708-1712 (2001).
- 6 Gudjonsson, T., Ronnov-Jessen, L., Villadsen, R., Bissell, M. J., Petersen, O. W. To create the correct microenvironment: three-dimensional heterotypic collagen assays for human breast epithelial morphogenesis and neoplasia. *Methods*. **30** (3), 247-255 (2003).
- 7 Pampaloni, F., Reynaud, E. G., Stelzer, E. H. The third dimension bridges the gap between cell culture and live tissue. *Nature Reviews in Molecular and Cell Biology*. **8** (10), 839-845 (2007).

701 8 Hirschhaeuser, F. et al. Multicellular tumor spheroids: an underestimated tool
702 is catching up again. *Journal of Biotechnology*. **148** (1), 3-15 (2010).

703 9 Jacobi, N. et al. Organotypic three-dimensional cancer cell cultures mirror drug
704 responses in vivo: lessons learned from the inhibition of EGFR signaling. *Oncotarget*. **8** (64),
705 107423-107440 (2017).

706 10 Rodriguez-Enriquez, S. et al. Energy metabolism transition in multi-cellular
707 human tumor spheroids. *Journal of Cell Physiology*. **216** (1), 189-197 (2008).

708 11 Kunz-Schughart, L. A. Multicellular tumor spheroids: intermediates between
709 monolayer culture and in vivo tumor. *Cell Biology International*. **23** (3), 157-161 (1999).

710 12 Andersen, A. P. et al. Roles of acid-extruding ion transporters in regulation of
711 breast cancer cell growth in a 3-dimensional microenvironment. *Molecular Cancer*. **15** (1),
712 45 (2016).

713 13 Swietach, P., Patiar, S., Supuran, C. T., Harris, A. L., Vaughan-Jones, R. D. The
714 role of carbonic anhydrase 9 in regulating extracellular and intracellular pH in three-
715 dimensional tumor cell growths. *Journal of Biological Chemistry*. **284** (30), 20299-20310
716 (2009).

717 14 Walenta, S., Doetsch, J., Mueller-Klieser, W., Kunz-Schughart, L. A. Metabolic
718 imaging in multicellular spheroids of oncogene-transfected fibroblasts. *Journal of*
719 *Histochemistry and Cytochemistry*. **48** (4), 509-522 (2000).

720 15 Kunz-Schughart, L. A., Groebe, K., Mueller-Klieser, W. Three-dimensional cell
721 culture induces novel proliferative and metabolic alterations associated with oncogenic
722 transformation. *International Journal of Cancer*. **66** (4), 578-586 (1996).

723 16 Feng, H. et al. Homogeneous pancreatic cancer spheroids mimic growth
724 pattern of circulating tumor cell clusters and macrometastases: displaying heterogeneity
725 and crater-like structure on inner layer. *Journal of Cancer Research and Clinical Oncology*.
726 **143** (9), 1771-1786 (2017).

727 17 Santini, M. T., Rainaldi, G., Indovina, P. L. Apoptosis, cell adhesion and the
728 extracellular matrix in the three-dimensional growth of multicellular tumor spheroids.
729 *Critical Reviews in Oncology/Hematology*. **36** (2-3), 75-87 (2000).

730 18 Vinci, M. et al. Advances in establishment and analysis of three-dimensional
731 tumor spheroid-based functional assays for target validation and drug evaluation. *BMC*
732 *Biology*. **10** 29 (2012).

733 19 Pickl, M., Ries, C. H. Comparison of 3D and 2D tumor models reveals enhanced
734 HER2 activation in 3D associated with an increased response to trastuzumab. *Oncogene*. **28**
735 (3), 461-468 (2009).

736 20 Wong, C., Vosburgh, E., Levine, A. J., Cong, L., Xu, E. Y. Human neuroendocrine
737 tumor cell lines as a three-dimensional model for the study of human neuroendocrine
738 tumor therapy. *Journal of Visual Experiments*. 10.3791/4218 (66), e4218 (2012).

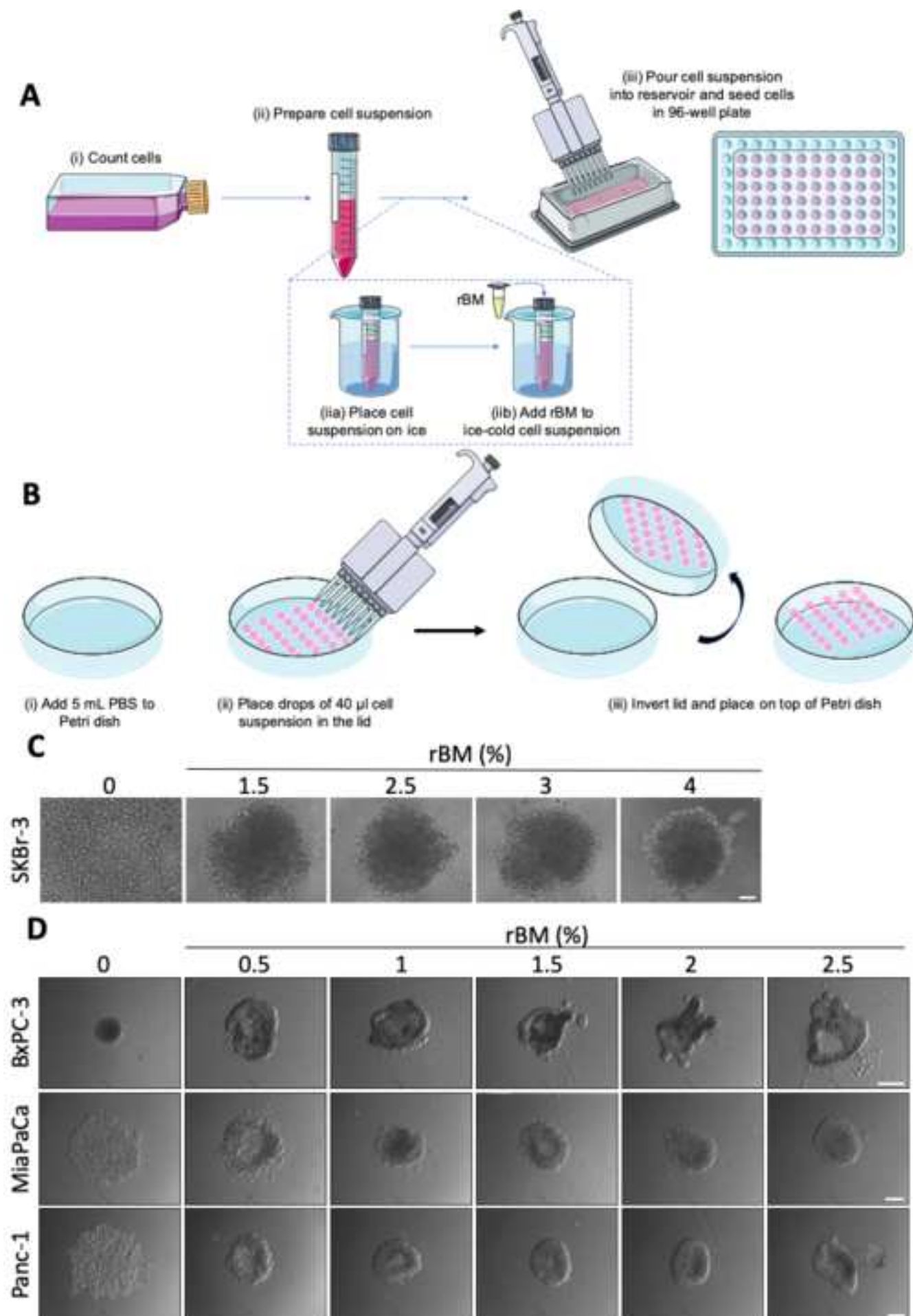
739 21 Friedrich, J. et al. A reliable tool to determine cell viability in complex 3-d
740 culture: the acid phosphatase assay. *Journal of Biomolecular Screening*. **12** (7), 925-937
741 (2007).

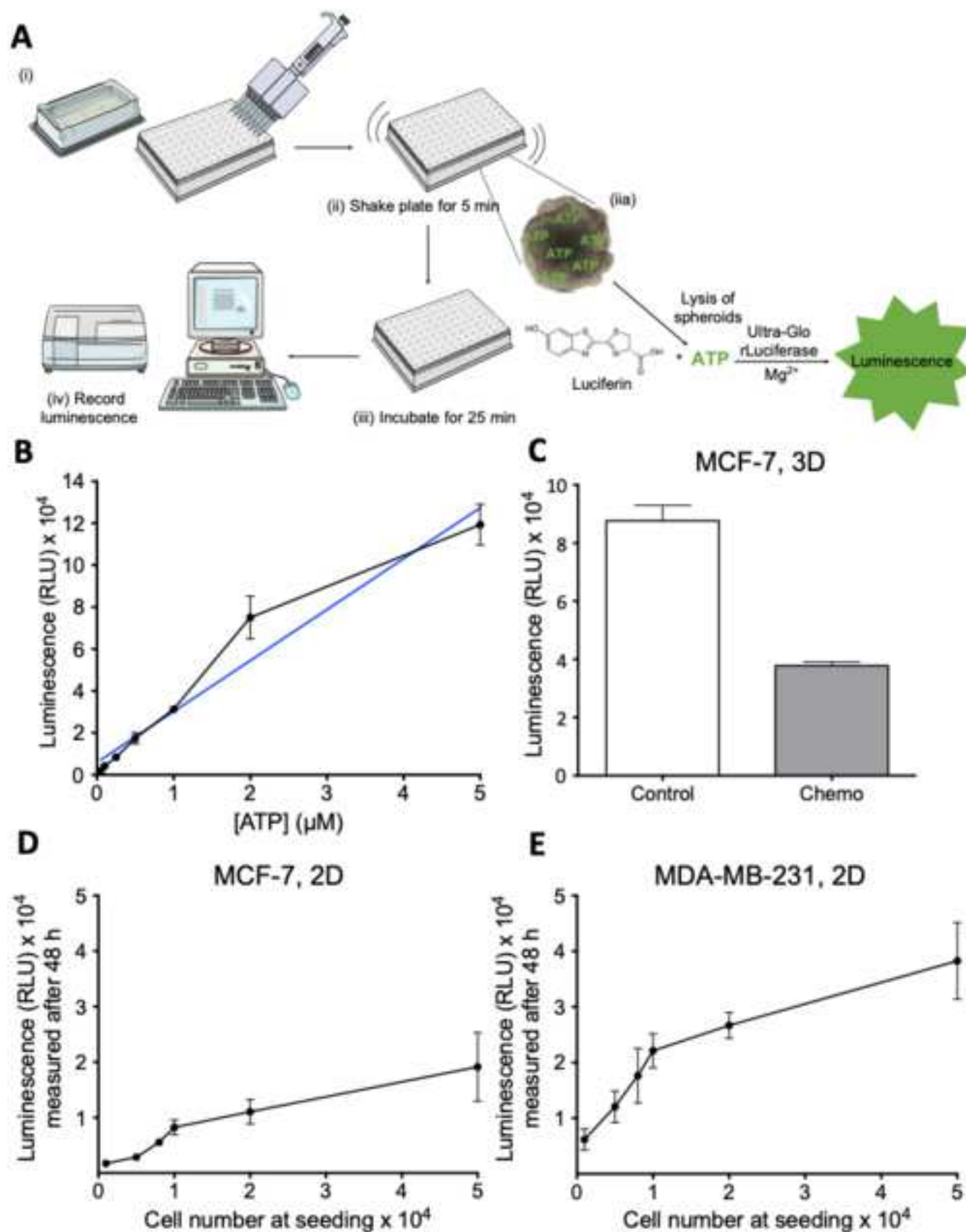
742 22 Ivascu, A., Kubbies, M. Diversity of cell-mediated adhesions in breast cancer
743 spheroids. *International Journal of Oncology*. **31** (6), 1403-1413 (2007).

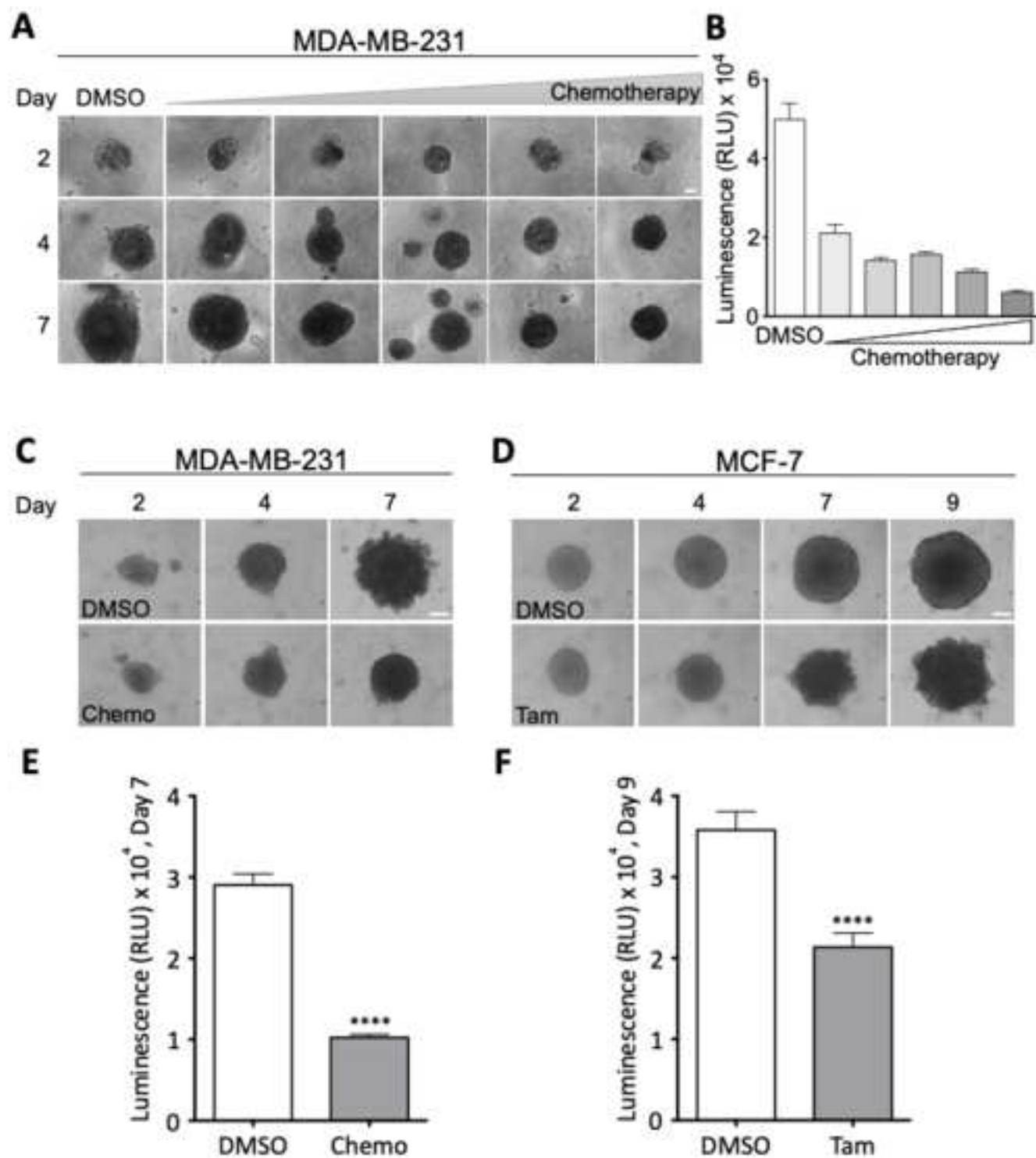
744 23 Crouch, S. P., Kozlowski, R., Slater, K. J., Fletcher, J. The use of ATP
745 bioluminescence as a measure of cell proliferation and cytotoxicity. *Journal of*
746 *Immunological Methods*. **160** (1), 81-88 (1993).

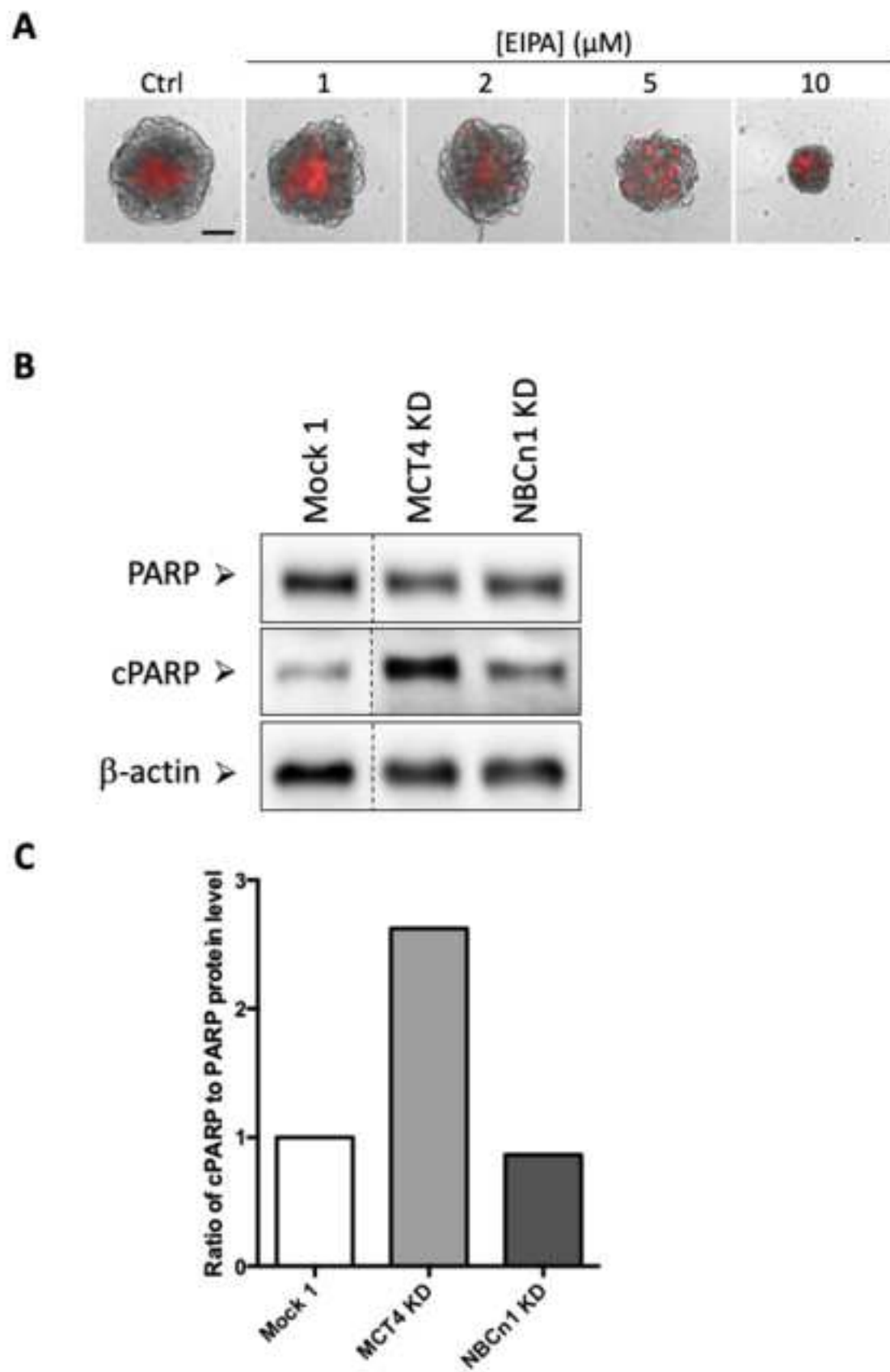
24 Andersen, A. P. et al. The net acid extruders NHE1, NBCn1 and MCT4 promote
 mammary tumor growth through distinct but overlapping mechanisms. *International
 Journal of Cancer*. (2018).
 25 Vaupel, P. Tumor microenvironmental physiology and its implications for
 radiation oncology. *Seminars in Radiation Oncology*. **14** (3), 198-206 (2004).
 26 Vaupel, P. W., Frinak, S., Bicher, H. I. Heterogeneous oxygen partial pressure
 and pH distribution in C3H mouse mammary adenocarcinoma. *Cancer Research*. **41** (5),
 2008-2013 (1981).
 27 Helmlinger, G., Yuan, F., Dellian, M., Jain, R. K. Interstitial pH and pO₂ gradients
 in solid tumors in vivo: high-resolution measurements reveal a lack of correlation. *Nature
 Medicine*. **3** (2), 177-182 (1997).
 28 Zhang, X., Lin, Y., Gillies, R. J. Tumor pH and its measurement. *Journal of
 Nuclear Medicine* **51** (8), 1167-1170 (2010).
 29 Gillies, R. J., Raghunand, N., Karczmar, G. S., Bhujwalla, Z. M. MRI of the tumor
 microenvironment. *Journal of Magnetic Resonance Imaging*. **16** (4), 430-450 (2002).
 30 Vukovic, V., Tannock, I. F. Influence of low pH on cytotoxicity of paclitaxel,
 mitoxantrone and topotecan. *British Journal of Cancer*. **75** (8), 1167-1172 (1997).
 31 Song, C. W., Griffin, R., Park, H. J. in *Cancer Drug Resistance* (ed B. A. Teicher)
 21-42 (Humana Press, 2006).
 32 Lotz, C. et al. Role of the tumor microenvironment in the activity and
 expression of the p-glycoprotein in human colon carcinoma cells. *Oncology Reports*. **17** (1),
 239-244 (2007).
 33 Sant, S., Johnston, P. A. The production of 3D tumor spheroids for cancer drug
 discovery. *Drug Discovery Today: Technologies*. **23**, 27-36 (2017).
 34 Stratmann, A. T. et al. Establishment of a human 3D lung cancer model based
 on a biological tissue matrix combined with a Boolean in silico model. *Molecular Oncology*. **8**
 (2), 351-365 (2014).
 35 Kuen, J., Darowski, D., Kluge, T., Majety, M. Pancreatic cancer cell/fibroblast
 co-culture induces M2 like macrophages that influence therapeutic response in a 3D model.
PLoS One. **12** (7), e0182039 (2017).
 36 Bochet, L. et al. Adipocyte-derived fibroblasts promote tumor progression and
 contribute to the desmoplastic reaction in breast cancer. *Cancer Research*. **73** (18), 5657-
 5668 (2013).
 37 Amann, A. et al. Development of a 3D angiogenesis model to study tumour -
 endothelial cell interactions and the effects of anti-angiogenic drugs. *Scientific Reports*. **7**
 (1), 2963 (2017).
 38 LaBonia, G. J., Ludwig, K. R., Mousseau, C. B., Hummon, A. B. iTRAQ
 Quantitative Proteomic Profiling and MALDI-MSI of Colon Cancer Spheroids Treated with
 Combination Chemotherapies in a 3D Printed Fluidic Device. *Analytical Chemistry*. **90** (2),
 1423-1430 (2018).
 39 Hulikova, A., Vaughan-Jones, R. D., Swietach, P. Dual role of CO₂/HCO₃⁻
 formula buffer in the regulation of intracellular pH of three-dimensional tumor growths.
Journal of Biological Chemistry. **286** (16), 13815-13826 (2011).
 40 Wallace, D. I., Guo, X. Properties of tumor spheroid growth exhibited by simple
 mathematical models. *Frontiers in Oncology*. **3**, 51 (2013).
 41 Michel, T. et al. Mathematical modeling of the proliferation gradient in
 multicellular tumor spheroids. *Journal of Theoretical Biology*. **458**, 133-147 (2018).

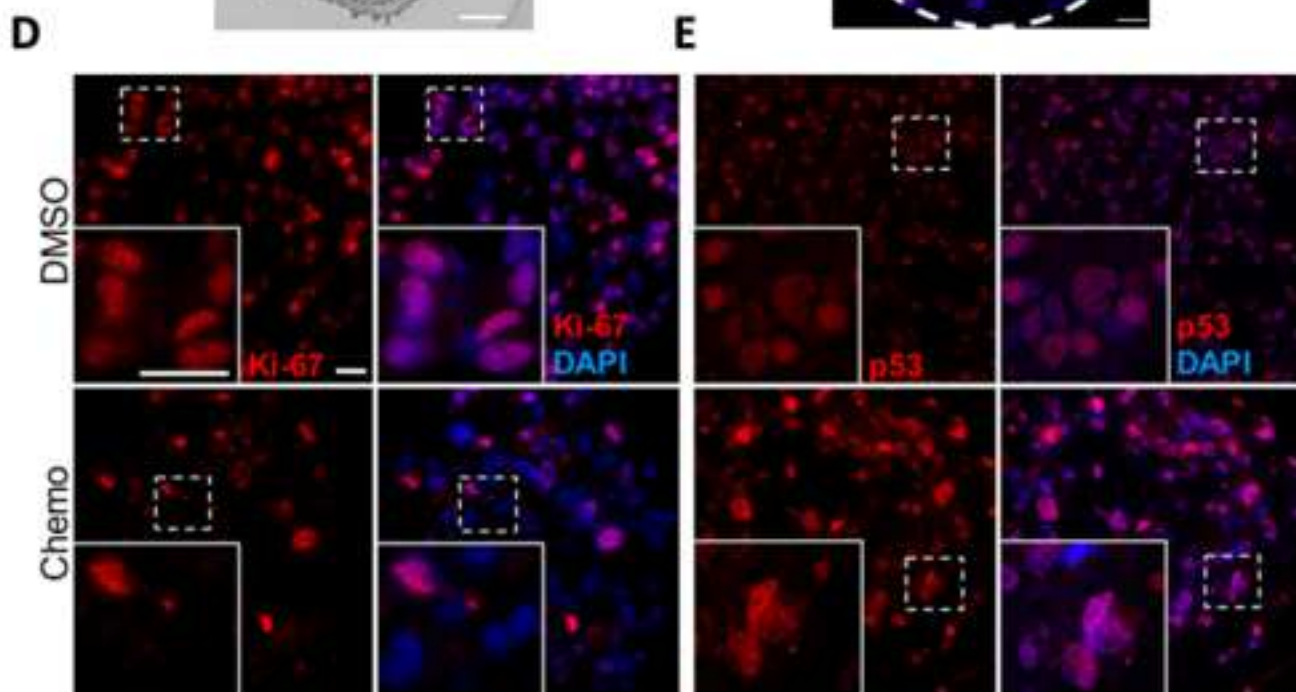
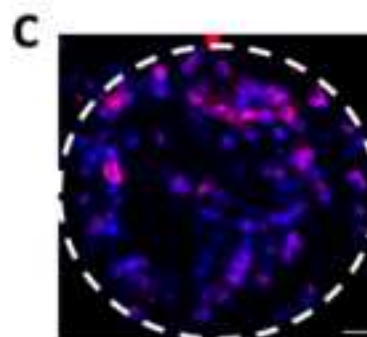
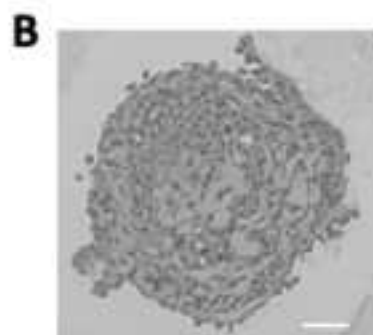
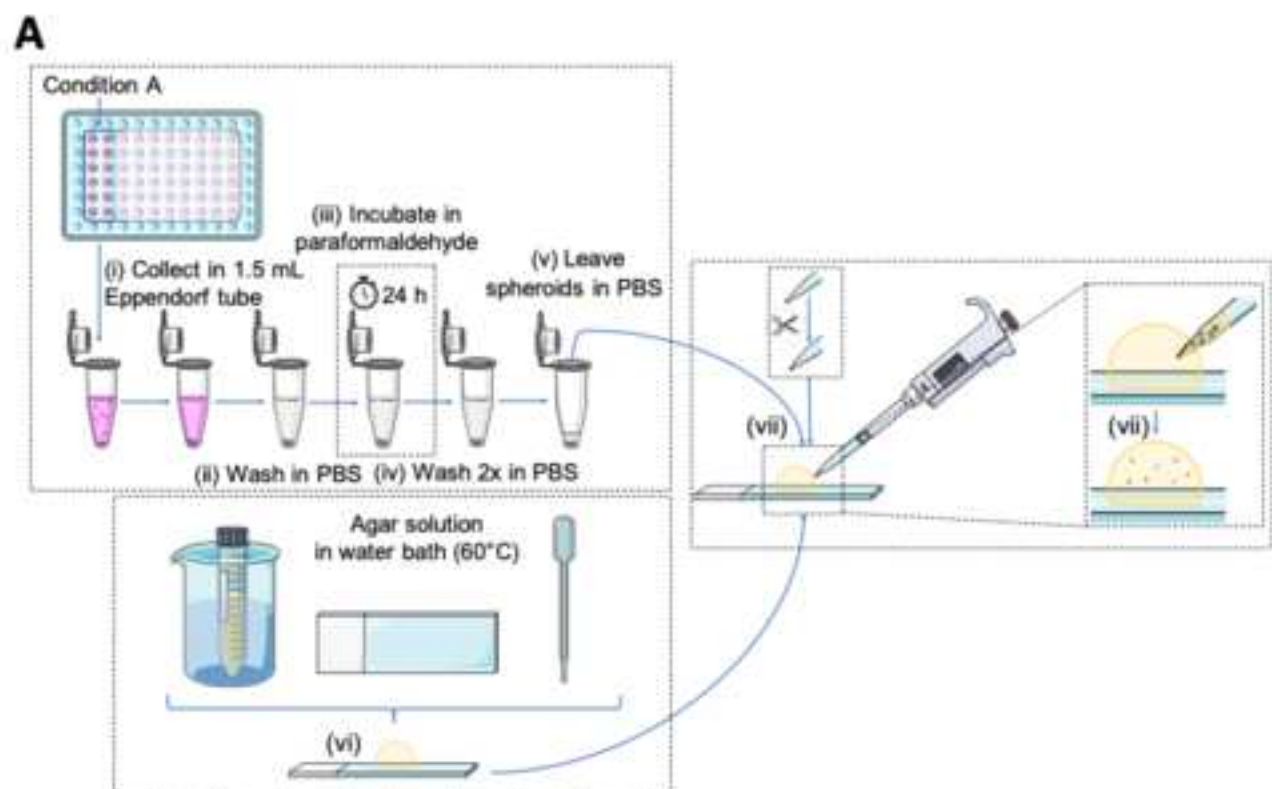
794 42 Meijer, T. G., Naipal, K. A., Jager, A., van Gent, D. C. Ex vivo tumor culture
795 systems for functional drug testing and therapy response prediction. *Future Science OA*. **3**
796 (2), FSO190 (2017).
797
798



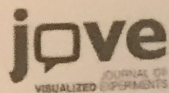








Name of material/equipment	Company	Catalog Number	Comments/Description
2-(4-aminophenyl)-1H-indole-6-carboxamide (DAPI)	Invitrogen	# C10595	For staining nuclei
5-Fluorouracil (5-FU)	Sigma-Aldrich	#F6627	Component in chemotherapeutic treatment
5-(N-ethyl-isopropyl) amiloride (EIPA)	Life Technologies	#E3111	Inhibitor of NHE1
Antibody against PARP and cPARP	Cell signaling	#9542	Used in western blotting
Antibody against Ki-67	Cell signaling	#9449	Used for IHC
Antibody against p53	Cell Signaling	#2524	Used for IHC
Antibody against β -actin	Sigma	A5441	Used in western blotting
Bactoagar	BD Bioscience	#214010	Used for agarose gel preparation
Benchmark protein ladder	Invitrogen	#10747-012	Used for SDS-PAGE
Bio-Rad DC Protein Assay kit	Bio-Rad Laboratories	#500-0113, #500-0114, #500-0115	Used for protein determination from lysates
Bürker chamber	Marienfeld	610311	For cell counting
BX63 epifluorescence microscope	Olympus		Used for fluorescent imaging
CellTiter-Glo 3D Cell Viability Assay	Promega	#G9681	Used for the cell viability assay
Cisplatin	Sigma-Aldrich	#P4394	Component in chemotherapeutic treatment
Corning Spheroid Microplate, 96 well, Black with clear round bottom, Ultra-low attachment, With lid, Sterile	Corning	#4520	Used for growing spheroids with luminescence measurements as end point
Corning 96 well, clear round bottom, Ultra-low attachment microplate, With lid, Sterile	Corning	#7007	Sufficient for spheroid growth without luminescence measurements as end point
Criterion TGX Precast Gels	Bio-Rad	5671025	Used for SDS-PAGE
Doxorubicin	Abcam	#120629	Component in chemotherapeutic treatment
FLUOStar Optima Microplate reader	BMG Labtech		Used for recording luminescence
Formaldehyde	VWR Chemicals	#9713.1000	Used for cell fixation
Geltrex LDEV-Free Reduced Growth Factor Basement Membrane Matrix	Gibco	#A1413202	Keep at 4 °C to prevent solidification. Referred to as rBM in the protocol.
Heat-inactivated FBS	Sigma	#F9665	Serum for growth media
ImageJ	NIH		Scientific Image analysis
Medim Uni-safe cassette	Medim Histotechnologie	10-0114	Used for storage of embedded spheroids
Mini protease inhibitor cocktail tablets	Roche Diagnostics GmBH	# 11836153001	Used for lysis buffer preparation
MZ16 microscope	Leica		Used for light microscopic images
NuPAGE LDS 4x Sample Buffer	Invitrogen	#NP0007	Used for western blotting
Pierce ECL Western blotting substrate	Thermo scientific	#32106	Used for western blotting
Ponceau S	Sigma-Aldrich	#P7170-1L	Used for protein band staining
Prism 6.0	Graphpad		Scientific graphing and statistical software
Propidium iodide (1mg/ml solution in water)	Invitrogen	P3566	Light sensitive
Sterile reservoirs, multichannel	SPL lifesciences	21002	Used for seeding cells for spheroid formation
Superfrost Ultra-Plus Adhesion slide	Menzel-Gläser	#J3800AMNZ	Microscope glass slide used for embedding
Tamoxifen	Sigma-Aldrich	#T5648	Used as chemotherapeutic treatment
Trans-blot Turbo 0.2 μ m nitrocellulose membranes	Bio-Rad	#170-4159	Used for western blotting
Tris/Glycine/SDS running buffer	Bio-Rad	#161 0732	Used for SDS-PAGE
Trypsin-EDTA solution	Sigma	#T4174	Cell dissociation enzyme



1 Alewife Center #200
Cambridge, MA 02140
tel. 617.945.9051
www.jove.com

ARTICLE AND VIDEO LICENSE AGREEMENT

Title of Article:

Assessing cell viability and death in 3D spheroid cultures of cancer cells

Author(s):

Michala G. Rolver, Line O. Elingaard-Larsen, Stine F. Pedersen

Item 1: The Author elects to have the Materials be made available (as described at <http://www.jove.com/publish>) via:

☒ Standard Access

☐ Open Access

Item 2: Please select one of the following items:

☒ The Author is **NOT** a United States government employee.

☐ The Author is a United States government employee and the Materials were prepared in the course of his or her duties as a United States government employee.

☐ The Author is a United States government employee but the Materials were NOT prepared in the course of his or her duties as a United States government employee.

ARTICLE AND VIDEO LICENSE AGREEMENT

1. **Defined Terms.** As used in this Article and Video License Agreement, the following terms shall have the following meanings: **"Agreement"** means this Article and Video License Agreement; **"Article"** means the article specified on the last page of this Agreement, including any associated materials such as texts, figures, tables, artwork, abstracts, or summaries contained therein; **"Author"** means the author who is a signatory to this Agreement; **"Collective Work"** means a work, such as a periodical issue, anthology or encyclopedia, in which the Materials in their entirety in unmodified form, along with a number of other contributions, constituting separate and independent works in themselves, are assembled into a collective whole; **"CRC License"** means the Creative Commons Attribution-Non Commercial-No Derivs 3.0 Unported Agreement, the terms and conditions of which can be found at: <http://creativecommons.org/licenses/by-nc-nd/3.0/legalcode>; **"Derivative Work"** means a work based upon the Materials or upon the Materials and other pre-existing works, such as a translation, musical arrangement, dramatization, fictionalization, motion picture version, sound recording, art reproduction, abridgment, condensation, or any other form in which the Materials may be recast, transformed, or adapted; **"Institution"** means the institution, listed on the last page of this Agreement, by which the Author was employed at the time of the creation of the Materials; **"JoVE"** means MyJoVE Corporation, a Massachusetts corporation and the publisher of The Journal of Visualized Experiments; **"Materials"** means the Article and / or the Video; **"Parties"** means the Author and JoVE; **"Video"** means any video(s) made by the Author, alone or in conjunction with any other parties, or by JoVE or its affiliates or agents, individually or in collaboration with the Author or any other parties, incorporating all or any portion

of the Article, and in which the Author may or may not appear.

2. **Background.** The Author, who is the author of the Article, in order to ensure the dissemination and protection of the Article, desires to have the JoVE publish the Article and create and transmit videos based on the Article. In furtherance of such goals, the Parties desire to memorialize in this Agreement the respective rights of each Party in and to the Article and the Video.

3. **Grant of Rights in Article.** In consideration of JoVE agreeing to publish the Article, the Author hereby grants to JoVE, subject to **Sections 4 and 7** below, the exclusive, royalty-free, perpetual (for the full term of copyright in the Article, including any extensions thereto) license (a) to publish, reproduce, distribute, display and store the Article in all forms, formats and media whether now known or hereafter developed (including without limitation in print, digital and electronic form) throughout the world, (b) to translate the Article into other languages, create adaptations, summaries or extracts of the Article or other Derivative Works (including, without limitation, the Video) or Collective Works based on all or any portion of the Article and exercise all of the rights set forth in (a) above in such translations, adaptations, summaries, extracts, Derivative Works or Collective Works and (c) to license others to do any or all of the above. The foregoing rights may be exercised in all media and formats, whether now known or hereafter devised, and include the right to make such modifications as are technically necessary to exercise the rights in other media and formats. If the "Open Access" box has been checked in **Item 1** above, JoVE and the Author hereby grant to the public all such rights in the Article as provided in, but subject to all limitations and requirements set forth in, the CRC License.

ARTICLE AND VIDEO LICENSE AGREEMENT

4. **Retention of Rights in Article.** Notwithstanding the exclusive license granted to JoVE in **Section 3** above, the Author shall, with respect to the Article, retain the non-exclusive right to use all or part of the Article for the non-commercial purpose of giving lectures, presentations or teaching classes, and to post a copy of the Article on the Institution's website or the Author's personal website, in each case provided that a link to the Article on the JoVE website is provided and notice of JoVE's copyright in the Article is included. All non-copyright intellectual property rights in and to the Article, such as patent rights, shall remain with the Author.

5. **Grant of Rights in Video – Standard Access.** This **Section 5** applies if the "Standard Access" box has been checked in **Item 1** above or if no box has been checked in **Item 1** above. In consideration of JoVE agreeing to produce, display or otherwise assist with the Video, the Author hereby acknowledges and agrees that, Subject to **Section 7** below, JoVE is and shall be the sole and exclusive owner of all rights of any nature, including, without limitation, all copyrights, in and to the Video. To the extent that, by law, the Author is deemed, now or at any time in the future, to have any rights of any nature in or to the Video, the Author hereby disclaims all such rights and transfers all such rights to JoVE.

6. **Grant of Rights in Video – Open Access.** This **Section 6** applies only if the "Open Access" box has been checked in **Item 1** above. In consideration of JoVE agreeing to produce, display or otherwise assist with the Video, the Author hereby grants to JoVE, subject to **Section 7** below, the exclusive, royalty-free, perpetual (for the full term of copyright in the Article, including any extensions thereto) license (a) to publish, reproduce, distribute, display and store the Video in all forms, formats and media whether now known or hereafter developed (including without limitation in print, digital and electronic form) throughout the world, (b) to translate the Video into other languages, create adaptations, summaries or extracts of the Video or other Derivative Works or Collective Works based on all or any portion of the Video and exercise all of the rights set forth in (a) above in such translations, adaptations, summaries, extracts, Derivative Works or Collective Works and (c) to license others to do any or all of the above. The foregoing rights may be exercised in all media and formats, whether now known or hereafter devised, and include the right to make such modifications as are technically necessary to exercise the rights in other media and formats. For any Video to which this **Section 6** is applicable, JoVE and the Author hereby grant to the public all such rights in the Video as provided in, but subject to all limitations and requirements set forth in, the CRC License.

7. **Government Employees.** If the Author is a United States government employee and the Article was prepared in the course of his or her duties as a United States government employee, as indicated in **Item 2** above, and any of the licenses or grants granted by the Author hereunder exceed the scope of the 17 U.S.C. 403, then the rights granted hereunder shall be limited to the maximum

rights permitted under such statute. In such case, all provisions contained herein that are not in conflict with such statute shall remain in full force and effect, and all provisions contained herein that do so conflict shall be deemed to be amended so as to provide to JoVE the maximum rights permissible within such statute.

8. **Protection of the Work.** The Author(s) authorize JoVE to take steps in the Author(s) name and on their behalf if JoVE believes some third party could be infringing or might infringe the copyright of either the Author's Article and/or Video.

9. **Likeness, Privacy, Personality.** The Author hereby grants JoVE the right to use the Author's name, voice, likeness, picture, photograph, image, biography and performance in any way, commercial or otherwise, in connection with the Materials and the sale, promotion and distribution thereof. The Author hereby waives any and all rights he or she may have, relating to his or her appearance in the Video or otherwise relating to the Materials, under all applicable privacy, likeness, personality or similar laws.

10. **Author Warranties.** The Author represents and warrants that the Article is original, that it has not been published, that the copyright interest is owned by the Author (or, if more than one author is listed at the beginning of this Agreement, by such authors collectively) and has not been assigned, licensed, or otherwise transferred to any other party. The Author represents and warrants that the author(s) listed at the top of this Agreement are the only authors of the Materials. If more than one author is listed at the top of this Agreement and if any such author has not entered into a separate Article and Video License Agreement with JoVE relating to the Materials, the Author represents and warrants that the Author has been authorized by each of the other such authors to execute this Agreement on his or her behalf and to bind him or her with respect to the terms of this Agreement as if each of them had been a party hereto as an Author. The Author warrants that the use, reproduction, distribution, public or private performance or display, and/or modification of all or any portion of the Materials does not and will not violate, infringe and/or misappropriate the patent, trademark, intellectual property or other rights of any third party. The Author represents and warrants that it has and will continue to comply with all government, institutional and other regulations, including, without limitation all institutional, laboratory, hospital, ethical, human and animal treatment, privacy, and all other rules, regulations, laws, procedures or guidelines, applicable to the Materials, and that all research involving human and animal subjects has been approved by the Author's relevant institutional review board.

11. **JoVE Discretion.** If the Author requests the assistance of JoVE in producing the Video in the Author's facility, the Author shall ensure that the presence of JoVE employees, agents or independent contractors is in accordance with the relevant regulations of the Author's institution. If more than one author is listed at the beginning of this Agreement, JoVE may, in its sole

ARTICLE AND VIDEO LICENSE AGREEMENT

discretion, elect not take any action with respect to the Article until such time as it has received complete, executed Article and Video License Agreements from each such author. JoVE reserves the right, in its absolute and sole discretion and without giving any reason therefore, to accept or decline any work submitted to JoVE. JoVE and its employees, agents and independent contractors shall have full, unfettered access to the facilities of the Author or of the Author's institution as necessary to make the Video, whether actually published or not. JoVE has sole discretion as to the method of making and publishing the Materials, including, without limitation, to all decisions regarding editing, lighting, filming, timing of publication, if any, length, quality, content and the like.

12. **Indemnification.** The Author agrees to indemnify JoVE and/or its successors and assigns from and against any and all claims, costs, and expenses, including attorney's fees, arising out of any breach of any warranty or other representations contained herein. The Author further agrees to indemnify and hold harmless JoVE from and against any and all claims, costs, and expenses, including attorney's fees, resulting from the breach by the Author of any representation or warranty contained herein or from allegations or instances of violation of intellectual property rights, damage to the Author's or the Author's institution's facilities, fraud, libel, defamation, research, equipment, experiments, property damage, personal injury, violations of institutional, laboratory, hospital, ethical, human and animal treatment, privacy or other rules, regulations, laws, procedures or guidelines, liabilities and other losses or damages related in any way to the submission of work to JoVE, making of videos by JoVE, or publication in JoVE or elsewhere by JoVE. The Author shall be responsible for, and shall hold JoVE harmless from, damages caused by lack of sterilization, lack of cleanliness or by contamination due to

the making of a video by JoVE its employees, agents or independent contractors. All sterilization, cleanliness or decontamination procedures shall be solely the responsibility of the Author and shall be undertaken at the Author's expense. All indemnifications provided herein shall include JoVE's attorney's fees and costs related to said losses or damages. Such indemnification and holding harmless shall include such losses or damages incurred by, or in connection with, acts or omissions of JoVE, its employees, agents or independent contractors.

13. **Fees.** To cover the cost incurred for publication, JoVE must receive payment before production and publication of the Materials. Payment is due in 21 days of invoice. Should the Materials not be published due to an editorial or production decision, these funds will be returned to the Author. Withdrawal by the Author of any submitted Materials after final peer review approval will result in a US\$1,200 fee to cover pre-production expenses incurred by JoVE. If payment is not received by the completion of filming, production and publication of the Materials will be suspended until payment is received.

14. **Transfer, Governing Law.** This Agreement may be assigned by JoVE and shall inure to the benefits of any of JoVE's successors and assignees. This Agreement shall be governed and construed by the internal laws of the Commonwealth of Massachusetts without giving effect to any conflict of law provision thereunder. This Agreement may be executed in counterparts, each of which shall be deemed an original, but all of which together shall be deemed to be one and the same agreement. A signed copy of this Agreement delivered by facsimile, e-mail or other means of electronic transmission shall be deemed to have the same legal effect as delivery of an original signed copy of this Agreement.

A signed copy of this document must be sent with all new submissions. Only one Agreement is required per submission.

CORRESPONDING AUTHOR

Name:

STINE FALSIG PEDERSEN

Department:

DEPARTMENT OF BIOLOGY

Institution:

UNIVERSITY OF COPENHAGEN

Title:

PROFESSOR

Signature:

Stine Falsig Pedersen

Date:

JAN 21, 2019

Please submit a **signed** and **dated** copy of this license by one of the following three methods:

1. Upload an electronic version on the JoVE submission site
2. Fax the document to +1.866.381.2236
3. Mail the document to JoVE / Attn: JoVE Editorial / 1 Alewife Center #200 / Cambridge, MA 02140

Manuscript Rolver et al JoVE59714

Point-by-point response to editor and reviewers

We thank the editor and reviewers for their constructive comments. A point-by-point response detailing the actions taken for each query is found below. A red-tracked version of the manuscript has been uploaded for review purposes, in addition to the clean, revised manuscript.

Editorial comments:

Changes to be made by the Author(s):

1. Please take this opportunity to thoroughly proofread the manuscript to ensure that there are no spelling or grammar issues. The JoVE editor will not copy-edit your manuscript and any errors in the submitted revision may be present in the published version.

2. Please remove all commercial language from your manuscript and use generic terms instead. All commercial products should be sufficiently referenced in the Table of Materials and Reagents. For example: Falcon tubes, Geltrex, Matrigel, ULA 96-well plates, Eppendorf, CellTiter-Glo 3D, etc.

Done

3. Please adjust the numbering of the Protocol to follow the JoVE Instructions for Authors. For example, 1 should be followed by 1.1 and then 1.1.1 and 1.1.2 if necessary. Please refrain from using bullets or dashes.

Done

4. Please revise the text to avoid the use of any personal pronouns in the protocol (e.g., "we", "you", "our" etc.).

Done

5. Please ensure that all text in the protocol section is written in the imperative tense as if telling someone how to do the technique (e.g., "Do this," "Ensure that," etc.). The actions should be described in the imperative tense in complete sentences wherever possible. Avoid usage of phrases such as "could be," "should be," and "would be" throughout the Protocol. Any text that cannot be written in the imperative tense may be added as a "Note." However, notes should be concise and used sparingly.

Done

6. The Protocol should contain only action items that direct the reader to do something.

We have rephrased to ensure that all protocol steps are action points

7. We cannot have non-numbered steps in the protocol. These should be either converted to a note or numbered action steps in imperative tense.

Done

8. Please provide volume and concentration of all the solutions used in the study.

Done

9. Software steps must be more explicitly explained ('click', 'select', etc.). Please add more specific details (e.g. button clicks for software actions, numerical values for settings, etc.).

For microscope settings we consider this meaningless as it would only be relevant for the precise microscope used. For ImageJ, we have added a link to the relevant protocol.

10. Please add more details to your protocol steps. Please ensure you answer the “how” question, i.e., how is the step performed?

Done

11. 1.1. What kind of cells or specific cell lines are used in the protocol?

Since the protocols are applicable for a wide range of cell lines, rather than specify directly in the protocol we have now added a note (p. 3-4), specifying which cell lines are, in our hands, most suited for each of the methods provided.

12. 1.2.5: How do you acquire the images? What magnification?

*We have now added (p. 4) the **Note:** The images in this paper are taken at 11.5x magnification, which is appropriate for most spheroids prepared using these protocols.*

13. There is a 10-page limit for the Protocol, but there is a 2.75-page limit for filmable content. Please highlight 2.75 pages or less of the Protocol (including headings and spacing) that identifies the essential steps of the protocol for the video, i.e., the steps that should be visualized to tell the most cohesive story of the Protocol.

Done

14. Each Figure Legend should include a title and a short description of the data presented in the Figure and relevant symbols. Please include a one liner title for all the panels combined in the figure legend.

Done.

15. For figure panels containing images from microscope, please include a scale bar and define it in the figure legend.

Done

16. Please obtain explicit copyright permission to reuse any figures from a previous publication. Explicit permission can be expressed in the form of a letter from the editor or a link to the editorial policy that allows re-prints. Please upload this information as a .doc or .docx file to your Editorial Manager account. The Figure must be cited appropriately in the Figure Legend, i.e. “This figure has been modified from [citation].”

Not relevant, all figures are new.

17. As we are a methods journal, please revise the Discussion to explicitly cover the following in detail in 3-6 paragraphs with citations:

- a) Critical steps within the protocol
- b) Any modifications and troubleshooting of the technique
- c) Any limitations of the technique
- d) The significance with respect to existing methods
- e) Any future applications of the technique

18. Please do not abbreviate the journal title in the references section.

19. Please alphabetically sort the materials table.

All the specific issues in query 17 have been addressed.

Reviewers' comments:

Reviewer #1:

Manuscript Summary:

In the present article, the authors described Three-dimensional (3D) spheroids of cancer cells are important tools for both cancer drug screens and for gaining mechanistic insight into cancer cell biology

They present here a series of simple methods for analysis of anti-cancer treatment-induced changes in cancer cell viability and death in 3D culture. The composition of the spheroids can be modified depending on the properties and biology of the cells employed, and the quantitative and qualitative analyses presented are useful both for assessing dose-response relationships and for gaining insight into the signaling- and death pathways involved. The efficacy of the protocol has been demonstrated, the authors show representative results analyzing pancreas mesenchymal phenotype and cell viability upon drug treatment. Thus, I recommend this manuscript for JoVE publication.

Reviewer #2:

Manuscript Summary:

Overall, this is a good JOVE manuscript describing spheroid formation techniques. I would recommend it for publication with minor clarification changes listed below.

Major Concerns:

None.

Minor Concerns:

-in the paragraph from line 85-96 I think that the authors should mention how spheroids or their proposed analysis assays fix these problems.

This point has now been clarified in this part of the introduction.

-line 111 state at what temperature, etc?

Now added (p. 4)

-line 114 growth medium with what percent serum? Growth medium without serum would not work to neutralize and growth medium with lower concentrations of serum might require more medium to neutralize.

6-10% serum depending on the cell line – now added in the protocol (point 1.1.3, p. 4).

-line 136 does "replace" mean that old medium is removed and fresh medium is added (as mentioned in several steps later in the protocol), or does it simply mean add fresh medium? This should maybe be clarified, since adding fresh medium on top of old medium without removing any could suffice as well.

The meaning has now been clarified at first mention (p. 4., 1.2.6), which now reads: "replace 100 μ L medium (remove 100 μ L and replace with 100 μ L fresh medium)".

-line 141 define LDEV

Done.

-line 165 be sure to define ULA as ultra-low attachment upon first mention of ultra-low attachment
Now done

-line 184/218 clarify what is meant by "replace" as mentioned for line 136
Has now been specified

-line 228 it is unclear which spheroid generation technique this analysis is based on. This is true for all analysis methods described in this paper. The authors should state that analysis techniques are described for "spheroid formation method 1" or "spheroids formed with ULA plates" or something like that because adding 100 uL of drug solution to a hanging droplet could be problematic.
Thank for pointing this out, this has now been specified throughout the protocols.

-For adding drug, why is it added at multiple time points? If one drug addition is not sufficient, clarify why.
This will depend on drug half-life, now specified (p. 7)

-line 262 do you wait for spheroids to settle, or do you spin them down?
They settle very quickly, centrifugation is not necessary. This has now been added to the text as a Note (page 8)

-line 268 what is meant by "if relevant"? When is it relevant and/or when is it not relevant?
Always relevant – now rephrased.

-line 270 how long does it take to settle? Why not centrifuge?
See above (line 262).

-line 279 does spin speed matter?
No, a quick spin using a tabletop centrifuge is sufficient. This has been added to the protocol (point 5.7, p. 9).

-line 300 reword "half to the volume"
Has been reworded

-line 306 is it necessary to cover while you incubate at room temp since (can light exposure affect luminescence readings?)
No, this is not necessary

-line 336 room temp should be defined as RT at first use
Done

-line 334 add "to fix" to this step in case a reader doesn't know the function of 4% paraformaldehyde
Now done

-line 340 in microwave or in the water bath
Has been rephrased

-line 330 clarify - each condition in a separate tube if that is the case

Thank you – has been clarified

-Section 5.2.8 is hard to follow. My comments on the section are as follows:

The whole section has been revised for clarity – see below for specific points.

-The step that needs to be done quickly should not include the cutting of the pipet tip as that could be done immediately before the time sensitive step, before time becomes an issue.

We agree, this point has been moved up (now 6.2.8, p. 10).

-Does PBS come into play in step II.? If so, please state in step II.

The spheroids are still in PBS at this step, but no additional PBS is used.

-"objective glass" is the glass on a microscope objective, in my understanding. Based on the corresponding figure I recommend rewording as "microscope slide" or "microscope glass"

Corrected

-If it is best to do step III. prior to step II., then step III and step II. should be swapped.

We agree – done.

-Wouldn't it be better to prop pipet vertically in a stand to minimize spheroids sticking to the side of the pipet tip? Wouldn't horizontal pipet placement encourage spheroids to settle onto the side of the tip due to gravity?

Because we, on your suggestion, have changed the order of steps II and III (albeit renumbered in the revised ms), this note is no longer necessary and has been removed.

-for step IV. It sounds like the authors mean to not penetrate the drop at all, but the corresponding figure suggests that they mean to not penetrate so far that the glass is hit. Please clarify.

This has been rephrased.

-line 371 couldn't this also happen if gelation is not complete?

Actually it would be impossible to push the drop off in this case.

-line 374 how long can/should they be stored in 70% EtOH?

Months, now added.

-line 385 1x or 10x PBS or does it not matter?

1xPBS – now added

-line 392 you should pre-warm it so you don't have to wait at this step

Agree, and this is actually what we do - corrected

-line 404 do you mean step 6.4?

Corrected (but numbering differs in the revised ms)

-step 6.7.II How is live/dead quantified from the z-projection? Is this done in ImageJ/Fiji? If so, what steps are taken in the software to accomplish this analysis? is the image exported to MATLAB

or something for analysis/quantification? Provide more details for this step so that readers can replicate.

We do not quantify the PI staining, as it is used for qualitative assessment of the localization of cell death. For quantitative analyses we use the described viability assay. To facilitate analysis for the reader, we have added a link to the relevant ImageJ instructions (p 8).

-line 435 this sentence should be the last sentence of the previous paragraph.

Corrected

-line 487 this sentence should be the last sentence of the previous paragraph.

Corrected

-Figure 4C/D Do you have lower magnification images for these showing the whole spheroid? it seems like the cells are very disperse and makes it look like these are stains of 2D culture instead of spheroids. Even if you just have the lower magnification images as an inset, might help make it clearer that you stained the embedded spheroids. Are scale bars correct (50 um in B and 20 um in C)? are both scale bars in C the same? Please clarify the scale bars in the phase and IF images.

Yes the scale bars are correct. The description in the figure legend has now been clarified.

-line 603-605 couldn't the matrigel contamination be fixed with a no spheroid matrigel control from the same batch of matrigel? Doesn't IHC also capture matrigel in the analysis?

In principle yes, but in our hands this is extremely difficult to control precisely enough to obtain sufficiently evenly loaded Western blots. In IHC this is not a problem unless of course specifically staining for matrix components.

Reviewer #3:

Manuscript Summary:

Three-dimensional (3D) culture of cancer cells better mimic the tumor microenvironment compared to two-dimensional (2D) culture and is an attractive tool to look at drug screening, cell proliferation, and protein expression in a 3D context, as opposed to traditional 2D plate culture. This manuscript describes three methods to grow cancer cells as 3D spheroids: 1. Hanging drop spheroids, 2. Spontaneous spheroid, and 3. Reconstituted basement membrane-mediated spheroids. In proof-of-concept examples, the authors demonstrate the applicability of 3D spheroids to look at drug penetration, cell proliferation/death (e.g. PI staining) and the ability to embed cultures in agar,

There is strong motivation and need for this protocol for the scientific community—can be an extremely helpful tool for those new to 3D culture. In general, the explanations and graphics are very easy to understand and well communicated. I appreciated the discussion where limitations are discussed (i.e. acid phosphatase assay) and alternative experiments are mentioned. My recommendation is to accept with minor recommendations.

Minor Concerns:

Comments/questions are provided in a point-by-point fashion:

1. In the introduction, the authors should be clearer at the last paragraph that there will be three types of culture methods discussed. Please edit accordingly.

Thank you – we have now introduced the sentence (p 3): Specifically, we provide and compare three different methods for spheroid formation, followed by methods for qualitative and quantitative analyses of growth, viability and drug response.

2. Can the authors comment on the differences between the three methods and how they could/should impact the applications described (e.g. will there be differences in cell proliferation or protein expression from lysates between the different culture methods?).

Now added to the Discussion, on p. 14.

3. The authors describe using 3D culture for proteins from cell lysates but to the best of my knowledge, did not provide any representative results. Why not—please comment.

Our fault, thank you for pointing this out. Has now been added as new Figure 4B-C.

4. Can the authors comment how drug screening, PI, or any of their applications differ between 3D culture and traditional 2D culture? Please comment

The overall principle of drug screening, PI staining, IHC and Western blotting are of course similar between 2D and 3D, as also indicated in the manuscript (e.g. protocol 5 – protein lysates and western blotting). The difference lies in the specific handling and procedures in 3D, and, of course, in the results!

5. In section 5, from 5.2.1. to 5.2.2, please clarify how many spheroids are to be pooled.

Done

6. In general, what is the minimum to maximum number of spheroids for each assay?

This has now been specified for each protocol (point 2.1, 3.1, 4.1, 5.1, 6.2.1)

Reviewer #4:

Manuscript Summary:

This paper discussed methodologies on assessing cell viability/death in a 3D spheroid cancer model. It listed 3 general approaches to forming 3D spheroids with cancer cells. Also it listed 3 different post culture analyses for cell viability. Overall, this is a well-written paper with detailed protocols enlisted. Please see additional comments below:

1. On page4, line 113-116, there is no centrifuge step after cell dissociation with enzyme. Do the authors centrifuge after dissociation? What is the speed and time?

No centrifugation step was used.

2. The authors introduced 3 ways of generating spheroids, 1) spontaneous spheroid formation; 2) reconstituted basement membrane mediated spheroid formation; 3) Hanging drop spheroid formation. Is there any difference in morphology or other genetic difference between the 3 approaches?

This has now been briefly discussed on p. 14 of the Discussion. As also noted in the Discussion (p. 14-15), the specific ability to generate spheroids is cell-type dependent, at least in part reflecting differential expression of cell-cell adhesion molecules.

3. In the 2nd approach of generating spheroids, it would help to have a brief explanation as to why one needs to centrifuging the plate after transferring cell suspensions/geltrex into 96 well plate. Will the centrifugation cause any unevenly distribution of cells in the geltrex?

This step will ensure that the cells are clustered together when the rBM hardens, facilitating formation of one single spheroid. This has now been added under point 1.3.11 (p 5).

4. In line 191 on page 5: does this contain a typo- 50,000 (50k) cells instead of 50.000 (50) cells per mL?

Thank you for pointing this out – this has been corrected!

5. For the hanging drop spheroids, it seems that the 2000 cells within each drop (40uL) are to survive and expand in 40uL medium. Is this enough nutrients for the cells considering they are expanding into spheroids?

Yes for the 4 days they are growing under these conditions, this appears to be sufficient. It may be noted that cells grown in 3D do not proliferate as much as cells in 2D, due to the inherent growth limitations in the spheroid core. Notably, this is part of the reason that this preparation resembles a tumor better than does a 2D preparation.

6. For the hanging drop spheroids, could the author provide more specific protocols on how to remove and transfer the spheroids into 96 well plate or other wells for drug screening or protein extraction assay after the spheroids are formed on the lid of the petri dish?

This has now been done – added on p. 6 as point 1.4.7.

To further clarify this point, we have also added the following sentence (p. 4.):

Note: *Three protocols each describing a different method for spheroid formation are presented below. Protocol 1.2 and 1.3 can be used for all the subsequent analytic protocols presented, whereas protocol 1.4 is best suited for embedding and lysate preparations. Depending on the cell line, spheroid formation takes 2-4 days, irrespective of the method used.*

7. On page 7, line 275, why is lysis buffer heated? Will the heat denature the protein sample?

This is standard procedure for this composition of lysis buffers, and will not harm the proteins.

8. It is understandable that estimating the cell number in spheroids may be challenging. However, is there any general rule of thumb that allows the size of spheroids to provide a general estimate of the cell number? Otherwise, how would one determine the cell number? The cell number would be useful when deciding how much lysis buffer, stain, etc are needed during post analysis.

Because cell size and spheroid tightness differ greatly between cell types, the size of the spheroid cannot be an indication of cell number. However, the cell viability assay in combination with imaging of spheroid size is useful for – within a given cell line and a given experiment – relating cell number to spheroid size (see Figure 2-3). A precise assessment of cell number can be made by dissociating the spheroids by trypsinization, followed by FACS analysis.

9. On page 8, line 336, does the gentle shaking during incubation help paraformaldehyde diffuse through the spheroids?

We actually find that shaking is not necessary to fix the spheroids fully under the conditions used.

10. On figure 1C-D, with increased rBM%, spheroids from certain cell types behaved differently. Is this due to the stiffness of the geltrax gel, or an indication that some cells are more sensitive to gel stiffness than others?

This is a very interesting question which cannot be answered from our experiments. However, it is well known that different cell types respond differently to matrix stiffness (e.g. ref (1-3)), so this is indeed a possibility.

11. In figure 3B, does the RLU of the different concentrations of chemotherapy differ significantly from one another? Could the concentration levels be included in the figure legend? Why is the 2nd lowest dose showing lower cell viability than the 3rd lowest dose?

The example shown is representative of 2 experiments only, thus statistical analysis is not relevant. The difference in RLU between the two doses mentioned presumably just reflects biological variation.

13. Based on the spherical size presented in Figure 3A, it would seem that the spheroid size does not substantially affect chemo-response in the higher chemo range? Would this be a reasonable interpretation and if so, is there an explanation?

The spheroid size at the onset of treatment is identical in the experiment shown (upper row, day 2). Thus, whether there is a difference in chemotherapy response with spheroid size cannot be inferred from this experiment.

14. Is it possible to use live/dead stain to differentiate the live/dead cells through microscopy in the spheroids?

Yes this is possible. As this protocol is slightly more expensive and time consuming we have chosen to only include the PI staining, which we find is generally sufficient.

15. Is it possible to dissociate the cells after the spheroid formed. After dissociating the cells, flow cytometry can be run to identify live/dead as well as other markers.

Yes, this is possible and is indeed done in some labs. For our purposes we find that the quantitative viability assay in conjunction with the other methods described is more practical and fully sufficient.

16. The authors include a protein extraction protocol in the paper. It would help to have a RNA/DNA extraction protocol from spheroids included as well.

We agree, however, given the length limitations on the JoVE protocols and the focus in this paper specifically on viability assessments, we have chosen not to include this.

References for this rebuttal letter

1. Jabbari E, Sarvestani SK, Daneshian L, Moeinzadeh S. Optimum 3D Matrix Stiffness for Maintenance of Cancer Stem Cells Is Dependent on Tissue Origin of Cancer Cells. PLoS One. 2015;10(7):e0132377.
2. Jiang T, Zhao J, Yu S, Mao Z, Gao C, Zhu Y, et al. Untangling the response of bone tumor cells and bone forming cells to matrix stiffness and adhesion ligand density by means of hydrogels. Biomaterials. 2019;188:130-43.
3. Nguyen-Ngoc KV, Cheung KJ, Brenot A, Shamir ER, Gray RS, Hines WC, et al. ECM microenvironment regulates collective migration and local dissemination in normal and malignant mammary epithelium. Proc Natl Acad Sci U S A. 2012;109(39):E2595-604.

Assessing cell viability and death in 3D spheroid cultures of cancer cells

Michala G. Rolver, Line O. Elingaard-Larsen, Stine F. Pedersen*

²*Section for Cell Biology and Physiology, Department of Biology, Faculty of Science,
University of Copenhagen, Copenhagen, Denmark*

Running title: Cell viability and death in 3D spheroids

Authors and institution/affiliation:

Michala G. Rolver

*Section for Cell Biology and Physiology,
Department of Biology, Faculty of Science
University of Copenhagen
Universitetsparken 13
DK-2100 Copenhagen, Denmark
cmh160@alumni.ku.dk*

Line O. Elingaard-Larsen

*Section for Cell Biology and Physiology,
Department of Biology, Faculty of Science
University of Copenhagen
Universitetsparken 13
DK-2100 Copenhagen, Denmark
jbq748@alumni.ku.dk*

*) Correspondence:

Stine F. Pedersen

*Section for Cell Biology and Physiology,
Department of Biology, Faculty of Science
University of Copenhagen
Universitetsparken 13
DK-2100 Copenhagen, Denmark
Email: sfpedersen@bio.ku.dk*

Key words: Spheroids, 3D cell culture, hanging drop, cell viability, breast cancer, pancreatic cancer, anti-cancer therapy, drug treatment, chemotherapy, reconstituted basement membrane, propidium iodide, immunohistochemistry.

Summary:

Here, we present several simple methods for evaluating viability and death in 3D cancer cell spheroids, which mimic the physico-chemical gradients of *in vivo* tumors much better than does 2D culture. The spheroid model therefore allows evaluation of cancer drug efficacy with improved translation to *in vivo* conditions.

Abstract

Three-dimensional ~~(3D)~~ spheroids of cancer cells are important tools for both cancer drug screens and for gaining mechanistic insight into cancer cell biology. The power of this preparation lies in its ability to mimic many aspects of the *in vivo* conditions of tumors, while being fast, cheap, and versatile enough to allow relatively high-throughput screening. The spheroid culture conditions can recapitulate the physico-chemical gradients in a tumor, including the increasing extracellular acidity, increased lactate, and decreasing glucose and oxygen availability, from the spheroid periphery to its core. Also the mechanical properties and cell-cell interactions of *in vivo* tumors are in part mimicked by this model. The specific properties and consequently the optimal growth conditions, of 3D spheroids differ widely between different types of cancer cells. Furthermore, the assessment of cell viability and death in 3D spheroids requires methods that differ in part from those employed for 2D cultures. Here we describe several protocols for preparing 3D spheroids of cancer cells, and for using such cultures to assess cell viability and death in the context of evaluating the efficacy of anticancer drugs.

Introduction

The use of multicellular spheroid models in cancer biology is several decades old ^{1,2}, but has gained substantial momentum in recent years. In large part, this reflects increased awareness of how strongly the phenotype of cancer cells is dependent on their microenvironment and specific growth conditions. The microenvironment in solid tumors is fundamentally different from that in corresponding normal tissues. This includes physico-chemical conditions such as pH, oxygen tension, as well as interstitial pressure, concentration gradients of soluble factors such as nutrients, waste products, and secreted signaling compounds (growth factors, cytokines). Furthermore, it includes the organization of the extracellular matrix (ECM), cell-cell interactions and intercellular signaling, and other aspects of the particular three-dimensional (3D) architecture of the tumor ³⁻⁶. The specific microenvironmental conditions, in which cancer cells exist, profoundly affects their gene expression profile and functional properties, and it is clear that, compared to that of cells grown in 2D, the phenotype of 3D spheroids much more closely mimics that of *in vivo* tumors ⁷⁻¹¹. 2D models, even if they employ hypoxia, acidic pH, and high lactate concentrations to mimic known aspects of the tumor microenvironment, still fail to capture the gradients of physico-chemical parameters arising within tumors, as well as their 3D tumor architecture. On the other hand, animal models are costly, slow, and ethically problematic, and generally also have shortcomings in their ability to recapitulate human tumor conditions. Consequently, 3D spheroids have been applied as an “intermediate complexity” model in studies of a wide range of properties of most solid cancers ^{9,11-17}.

A widely employed use of 3D spheroids is in screening assays of anticancer therapy efficacy ^{9,18-20}. Treatment responses are particularly sensitive to the tumor microenvironment, reflecting both the impact of the tortuosity, restricted diffusion, high interstitial pressure, and acidic environmental pH on drug delivery, and the impact of hypoxia and other aspects of the microenvironment on the cell death response ^{9,17}. Because the environment within 3D spheroids inherently develops all of these properties in this setting⁷⁻¹¹, employing 3D cell cultures can substantially improve the translation of results to *in vivo* conditions, ~~by partially recapitulating these conditions~~, yet allowing efficient and affordable high-throughput screening of net growth. However, the great majority of studies on the drug response of cancer cells are still carried out under 2D conditions. This likely reflects that, while some assays can relatively easily be implemented for 3D cell cultures, many, such as viability assays, ~~w~~Western blotting, and immunofluorescence analysis, are much more conveniently done in 2D than in 3D.

The aim of the present work is to provide easily amenable assays and precise protocols for analyses of the effect of treatment with anti-cancer drugs on cancer cell viability and survival in a 3D tumor mimicking setting. Specifically, we provide and compare three different methods for spheroid formation, followed by methods for qualitative and quantitative analyses of growth, viability and drug response.

Protocols

1. Generation of spheroids

1.1. Preparing cell suspensions for spheroid formation

Note: Different cell lines have very different adhesion properties and the most suitable spheroid formation protocol has to be established in each case. In our hands, MCF-7, and BxPC-3 ~~xxx, xxx and xx~~ cells are suitable for spontaneous spheroid formation, while MDA-MB-231, SKBr-3, Panc-1 and MiaPaCa require addition of reconstituted basement membrane to successfully form spheroids. We have so far only employed MDA-MB-231 and BxPC-3 cells for the hanging drop protocol, however other cell lines are ~~surely~~ certainly applicable. ~~xx, and xx, xx and xx for xx.~~

1.1.1. Grow cells as monolayer until 70-80% confluency.

1.1.2. Wash cells with phosphate buffered saline (~~PBS1~~ X PBS, 5 mL for a 25 cm² or 10 mL for a 75 cm² flask), add cell dissociation enzyme (0.5 mL for a 25 cm² or 1 mL for a 75 cm² flask) and incubate the cells for 2-5 min. ~~(37 °C, 5% CO₂, 95% humidity).~~

1.1.3. Check cell detachment under a microscope and neutralize cell dissociation enzyme by adding growth medium ~~(6-10% serum depending on the cell line)~~ to a total volume of 5 mL in a 25 cm² or 10 mL for a 75 cm² flask.

1.1.4. Count cells (Figure 1A, (i)). ~~We u~~Use a Bürker chamber and count 8 squares in the chamber per cell preparation to obtain a high reproducibility of the size of the spheroids.

~~Below we will present t~~Three protocols each describing a different method for spheroid formation ~~are presented below.~~

Note: Three protocols each describing a different method for spheroid formation are presented below. ~~Method~~Protocol 1.2 and 1.3 ~~2~~ can be used for all the subsequent analytic protocols presented, whereas ~~Method~~protocol 1.4 ~~3~~ is best suited for embedding and lysate preparations. ~~Depending on the cell line, spheroid formation takes 2-54 days, irrespective of the method used.~~

1.2. Spontaneous spheroid formation

1.2.1. Perform steps 1 ~~4 as described in.~~ 1.1. ~~1.1.4.~~

1.2.2. Dilute the cell suspension in a ~~Falcon~~ 15 mL tube to obtain 0.5-2 x 10⁴ cells/mL (optimal cell density needs to be determined for each cell line) (Figure 1A, (ii)).

1.2.3. Transfer cell suspension to a sterile reservoir and, using a multichannel pipette, dispense 200 µL/well into ultra-low attachment ~~(ULA)~~ 96-well round bottom plates (Figure 1A, (iii)). ~~It is advisable f~~to fill the outer ring of wells with ~~PBS1~~ X PBS or growth medium to reduce evaporation from the remaining wells.

1.2.4. Incubate the plate in an incubator (37 °C, 5% CO₂, 95% humidity).

1.2.5. Every 2-3 days, acquire light microscopic images of the spheroids.

Note: The images in this paper are taken at 11.5x magnification, which is appropriate for most spheroids prepared using these protocols.

1.2.6. Every 2-3 days (after acquiring images) replace 100 μ L medium (remove 100 μ L and replace with 100 μ L fresh medium). ~~and acquire images for evaluation of spheroid growth.~~

Note: To avoid removing spheroids when replacing medium, it is advisable to tilt the plate a bit while slowly removing the medium and inspect the aspirated medium in the tips for visible spheroids before discarding it.

~~Depending on the cell line, spheroid formation takes 2-5 days.~~

1.3. Reconstituted basement membrane-mediated spheroid formation.

Notice: ~~In our lab we~~ We use lactose dehydrogenase elevating virus (LDEV)-free, reduced growth factor ~~Geltrex as~~ reconstituted basement membrane (rBM), ~~but obviously Matrigel or other similar basement membrane products, or indeed specific extracellular matrix factors may be used.~~ rBM ~~Geltrex~~ is temperature-sensitive and should always be kept on ice, as it will clot if it reaches 15 °C. ~~If employing Geltrex, t~~Thaw the rBM ~~it~~ on ice either overnight at 4 °C or 2-4 h at room temperature (RT) before plating.

1.3.1. Thaw rBM ~~Geltrex~~ on ice (see Table of Material and reagents).

1.3.2. Keep plates and reservoirs (if individually wrapped) on ice before use.

1.3.3. Perform steps 1-4 ~~as described in 1.1.-1.1.4.~~

1.3.4. Dilute the cell suspension in a Falcon 15 mL tube to obtain $0.5-2 \times 10^4$ cells/mL (optimal cell density needs to be determined for each cell line) (Figure 1A, (ii)).

1.3.5. Place the 15 mL Falcon tube containing the diluted cell suspension on ice (e.g. in glass beaker) (Figure 1A (iia)).

1.3.6. Transfer the chilled plates and reservoirs to the hood. ~~It is advisable to~~ rinse plastic containers and fill them with ice and transfer them into the hood to allow the plates and reservoirs to be placed on ice during the entire procedure.

1.3.7. ~~Add 1-2% Geltrex (optimal concentration needs to be determined for each cell line) to the chilled cell suspensions immediately before transferring the cell suspension to a sterile reservoir and dispense 200 μ L/well into ULA 96 well plates using a multichannel pipette (Figure 1A, (iib) + (iii)).~~

1.3.7. Resuspend rBM gently to ensure a homogenous gel.

1.3.8. Add 1-2% rBM (optimal concentration needs to be determined for each cell line) to the chilled cell suspensions (Figure 1A (iib)).

1.3.9. Invert the 15 ml tube ~~tube~~ to ensure proper mixing of rBM and cell suspension before dispensing the suspension into the plate.

1.3.10. Transfer the rBM-containing cell suspension to a sterile reservoir and dispense 200 μ L/well into chilled ultra-low attachment 96-well plates using a multichannel pipette (Figure 1A (iii)).

Note: If working with several cell suspensions (e.g. more than one cell line), it is essential to dispense each cell suspension immediately after rBM addition to prevent premature gelling.

1.3.11. Centrifuge the plate for 15 min at 750 RCF (if possible at 4 °C to keep the rBM fluid longer, but not a requirement for successful spheroid formation), to ~~to~~. This will ensure that the cells are clustered together when the rBM hardens, facilitating formation of one single spheroid.

Before adding Geltrex to the cell suspension, resuspend the Geltrex gently to ensure a homogenous gel.

After Geltrex has been added, invert the Falcon tube to ensure proper mixing of Geltrex and cell suspension before dispensing the suspension into the plate.

If working with several cell suspensions (e.g. more than one cell line), it is essential to dispense each cell suspension immediately after Geltrex addition to prevent premature gelling.

1.3.8. After having transferred the cell suspensions to ULA 96-well plates, centrifuge the plate for 15 min. at 750 RCF (if possible at 4 °C to keep the Geltrex fluid longer, but not a requirement for successful spheroid formation).

1.3.9~~12~~. Incubate the plate in an incubator (37 °C, 5% CO₂, 95% humidity).

1.3.10~~3~~. Every 2-3 days, acquire light microscopic images for evaluation of spheroid growth replace 100 μ L medium and acquire images for evaluation of spheroid growth. Depending on the cell line, spheroid formation takes 2-5 days.

1.3.14. Every 2-3 days replace 100 μ L medium (remove 100 μ L and replace with 100 μ L fresh medium).

1.4. Hanging drop spheroids.

1.4.1. Perform step 1-4 as described in 1.1.1.4.

1.4.2. Dilute cells to obtain a suitable dilution. ~~We generally use~~ A practical dilution is 50,000 cells/mL.

1.4.3. Remove the lid of a 10 cm² ~~Petri cell culture~~ dish and place it so it faces upwards. Add 6 mL of ~~PBS1 X PBS~~ to the ~~Petri~~ dish (Figure 1B, (i)).

1.4.4. Pour the cell suspension into a sterile reservoir and carefully place up to 30 drops of 40 µL of cell suspension onto the lid of the cell culture Petri dish using a multichannel pipette (Figure 1B, (ii)), resulting in a concentration of 2000 cells/drop. There is room for at least 5 rows of 6 drops giving 30 spheroids per Petri dish. Avoid placing the drops too close to the edge of the lid as these drops are more likely to lose surface tension when inverting the lid in the following step.

1.4.5. Invert the lid in a quick but controlled movement and place it on top of the ~~PBS1 X PBS-containing Petri cell culture~~ dish (Figure 1B, (iii)).

1.4.6. Place the ~~Petri~~ dish in an incubator (37 °C, 5 % CO₂, 95 % humidity) without disturbing the drops, and leave them to grow for 4-6 days.

1.4.7. If to be used for protein lysates or embedding, pool spheroids by removing the lid and tilt it, in order to wash down the drops with 1 mL heated media. Transfer the resulting media containing spheroids to a 1.5 mL tube and allow them to settle to the bottom of the tube. Proceed as described in 5.4 and 6.2.2 for protein lysates and embedding, respectively.

2. Drug treatment of spheroids

Note: Long-term drug treatment can be applied to the spheroids in order to screen for effects of a drug of interest. Before initiating drug treatment, it is advisable to perform a dose response experiment of the drug(s), in order to find an appropriate dose for the experimental treatment. The doses should be based on the determined IC₅₀/K_i of the drug and range from around 0.2x-10x of this value.

2.1. Set up 6-12 spheroids per desired condition as described in 1.2 or 1.3 and place in incubator (37 °C, 5% CO₂, 95% humidity) for 2 days.

2.2. On day 2, take light microscopic images of the spheroids.

2.3. ~~P~~repare first treatment doses (after acquiring images).

Note: The first treatment concentration must be twice the desired final concentration as the solution will be diluted 1:2 upon addition to the well containing 100 µL medium. Suggested drug treatment intervals (will depend on drug half-life): Day 2, 4 and 7.

2.4. Using a multichannel pipette, gently remove 100 µL medium and replace it with 100 µL drug containing medium. Long-term drug treatment can be applied to the spheroids in order to screen for effects of a drug of interest.

~~Before initiating drug treatment, it is advisable to perform a dose response experiment of the drug(s), in order to find an appropriate dose for the experimental treatment. The doses should be based on the determined IC_{50}/K_i of the drug and range from around $0.2 \times 10 \times$ of this value.~~

~~2.1. Drug treatment frequency will depend on the drug half life, but we generally replace medium and drugs every 2-3 days. The first drug treatment can be given at day 2, where spheroids have formed.~~

~~2.2. Before drug treatment, acquire light microscope images of the spheroids in order to document initial size and visualize effects of the drug. It is advisable to require images of at least 3 spheroids per condition.~~

~~2.3. Mix the drug of interest to the desired concentration by diluting stock in medium.~~

~~100 μ L of the solution is needed per drug treated well.~~

~~In the first treatment the drug concentration should be twice the desired final concentration, as the solution will be diluted 1:2 upon addition to the well containing 100 μ L medium.~~

~~2.4. Remove 100 μ L medium (half the volume in the well) and add 100 μ L of the drug treatment solution.~~

~~In general, to avoid removing spheroids when having to discard a fraction of the medium, it is advisable to tilt the plate a bit while slowly removing the medium, and to inspect the aspirated medium (in the tips) for visible spheroids before discarding it.~~

~~2.5. Place the 96-well plate back in the incubator (37 °C, 5% CO₂, 95% humidity) and repeat 2.3 and 2.4 on the chosen days of treatment (but now without doubling the dose to obtain correct final dose)~~repeat this procedure every 2-3 days. Suggested drug treatment intervals (will depend on drug half life): Day 2, 4 and 7.~~~~

2.6. On the final day of the protocol/treatment schedule, one or several of the following assays can be performed.

~~2.6. On the final day of the desired length of drug treatment one or several of the assays described below can be performed.~~

3. Preparing protein lysates from 3D spheroid culture

It is advisable to use a P200 pipette and cut the end of the tip to allow a bigger opening and hence an easier capture of the spheroids without disturbing the spheroid structure.
3.1. Pool spheroids from each condition in a 1.5 mL Eppendorf tube.

~~It is advisable to use a P200 pipette and cut the end of the tip to allow a bigger opening and hence an easier capture of the spheroids without disturbing the spheroid structure.~~

~~2 mL Eppendorf tubes should not be used as the next steps will become more difficult due to their less pointy bottom.~~

~~If collecting a large number of spheroids, the amount of medium may exceed 1.5 mL before having collected all the spheroids. In that case, allow the collected spheroids to settle at the bottom and discard e.g. half the volume of the Eppendorf tube before continuing collecting the remaining spheroids.~~

~~3.2. Place tubes on ice and allow the spheroids to settle at the bottom of the Eppendorf tube.~~

~~3.3. If relevant, move from sterile cell laboratory to regular laboratory.~~

~~3.4. Wash twice in ice cold PBS. Let spheroids settle before removing PBS between each washing step.~~

~~3.5. Aspirate as much PBS as possible without disturbing or removing the spheroids.~~

~~3.6. Add 5 μ L heated lysis buffer (LB) with phosphatase and protease inhibitors, per spheroid (e.g. 10 spheroids = 50 μ L LB).~~

~~3.7. Repeat intervals of vortex followed by spin down until spheroids are dissolved. Perform a cycle of vortex for 30 s followed by centrifuge for 10 s for approx. 5–10 min depending on the size and the compactness of the spheroids.~~

~~**Note:** The protocol can be paused here. Keep the lysates at -20°C until proceeding with sonication, homogenization and protein determination as in a standard 2D lysate protocol.~~

~~4. Cell viability assay for spheroids – CellTiter Glo 3D~~

~~**3.** The cell viability assay, CellTiter Glo 3D, was chosen based on its simple and time efficient protocol and high reproducibility. Furthermore, this assay does not require complete removal of culture medium which is an advantage when working with spheroids. Other cell viability assays such as the acid phosphatase assay²⁴ can also be employed as long as they are adaptable to 3D cell cultures (see Discussion).~~

~~34.1. Set up 4-6 spheroids per desired condition as described in 1.2 or 1.3 and place in incubator (37°C , 5% CO_2 , 95% humidity).~~

~~**Note:** We perform the cell viability assay on day 7 or 9, after having monitored spheroid growth every 2-3 days by light microscopy as described above (point 1.2.5 and 1.3.13).~~

~~34.12. Thaw the CellTiter Glo 3D viability assay reagent (see Table of materials and reagents) and let it equilibrate to RT prior to use. The thawed reagent can be placed in a 22°C water~~

~~bath for approx. 30 min to equilibrate to RT.~~

~~34.32.~~ Mix gently by inverting to obtain a homogeneous solution.

~~34.43.~~ Before performing the assay, remove 50% of the culture medium from the spheroids (100 μ L).

~~34.54.~~ Add ~~a volume of CellTiter Glo 3D cell viability reagent half to the volume of to cell culture medium present in each well~~ at a {1:3} ratio to the amount of medium present in the well (Figure 2A, (i)). E.g. for a 96-well plate, add 50 μ L of ~~CellTiter Glo 3D~~ reagent to 100 μ L medium.

~~34.65.~~ Mix the contents vigorously for 5 min to induce cell lysis (Figure 2A, (ii)).

~~34.76.~~ Incubate for 25 min at RT to stabilize luminescent signal (Figure 2A, (iii)).

~~34.87.~~ Record luminescent signal (Figure 2A, (iv)).

4. Propidium Iodide (PI) staining of spheroids

~~46.1.~~ Set up 3-6 spheroids per desired condition as described in 1.2 or 1.3 and place in incubator (37 °C, 5% CO₂, 95% humidity).

~~46.2.~~ In a sterile cell culture lab, heat ~~1 x PBS~~ 1 X PBS to 37 °C.

~~46.3.~~ Make a PI solution of 4 μ M by diluting stock solution in ~~1 x PBS~~ 1 X PBS: Dilute a 1 mg/mL aqueous stock of PI 1:350 in 1 X PBS.

Note: This concentration will be further halved upon addition of the solution to the wells giving a final concentration of 2 μ M. 100 μ L of this solution is needed for each well containing a spheroid.

CAUTION: Propidium iodide (PI) must be handled in a fume hood and wearing gloves. PI is light sensitive. Protect from light when handling.

~~46.4.~~ Remove 100 μ L of the medium from each well in the 96-well plate without removing the spheroids.

~~46.5.~~ Wash out the remaining medium by adding 100 μ L of heated 1 X PBS to all wells followed by removing 100 μ L of the liquid in the wells. Repeat this washing step 3 times.

~~46.6.~~ Add 100 μ L of the PI solution to each well, cover the plate in aluminum foil and place it in an incubator (37 °C, 5% CO₂, 95% humidity) for 10-15 min.

~~46.7.~~ Repeat the 3 washing steps described in 46.5 to wash out PI solution, in order to diminish background signal when imaging.

46.8. Use an epifluorescence microscope to image the spheroids. To evaluate the viability of cells in the spheroid core take z-stacks to get images with varying depths of the spheroid.

Note: A step size around 18-35 μm between each slice depending on spheroid size is advisable, giving approximately 11-18 stacks per spheroid.

6.9. Z-stacks can be processed in ImageJ using the z-projection function, which can combine all z-stacks into one final picture, giving an overview of the staining throughout the spheroid (for further guidelines on the use of ImageJ for this purpose, see <https://imagej.net/Z-functions>).

5. Preparing protein lysates for western blotting from 3D spheroid cultures

Note: When collectingFor handling the spheroids, it is advisable to use a P200 pipette and cut the end of the tip to allow a bigger opening and hence an easier capture of the spheroids without disturbing their structure.

53.1. For each condition, pool a minimum of 12, ideally 18-24 spheroids (depending on spheroid size) in a 1.5 mL tube (avoid 2 mL tubes, as the next steps will become more difficult due to their less pointy bottom).

Note: If the amount of medium exceeds 1.5 mL before having collected all the spheroids, allow the collected spheroids to settle at the bottom (happens very quickly, centrifugation not necessary) and discard e.g. half the volume of the tube before continuing collecting the remaining spheroids.

53.2. Place tubes on ice and allow the spheroids to settle at the bottom of the 1.5 ml tube.

53.3. Move from sterile cell laboratory to regular laboratory.

53.4. Wash twice in 1 mL ice-cold PBS1 X PBS. Let spheroids settle before removing PBS1 X PBS between each washing step.

53.5. Aspirate as much PBS1 X PBS as possible without disturbing or removing the spheroids.

53.6. Add 5 μL heated lysis buffer (LB) with phosphatase- and protease inhibitors, per spheroid (e.g. 10 spheroids = 50 μL LB).

53.7. Repeat intervals of vortex followed by spin down until spheroids are dissolved. Perform a cycle of vortexing for 30 s followed by centrifugation (a quick spin using a tabletop centrifuge is sufficient) for 10 s for approx. 5-10 min depending on the size and the compactness of the spheroids.

Note: The protocol can be paused here. Keep the lysates at -20 $^{\circ}\text{C}$ until proceeding with sonication, homogenization and protein determination as in a standard 2D protein lysate protocol, followed by western blotting using standard protocols.

5.6. Embedding of 3D spheroids

6.1. Prepare the agarose gel into which the spheroids are embedded (only necessary first time performing the protocol).

6.1.1. Mix 1 g bactoagar in 50 mL ddH₂O.

6.1.2. Heat slowly in microwave oven until the bactoagar has dissolved and a homogenous gel has formed. The gel must not be allowed to boil.

6.1.3. Keep warm in a water bath at 60 °C.

6.1.4. Keep at 4 °C between experiments.

65.1 Preparation (first time)

65.1.1. Make the agarose gel into which the spheroids are embedded:

Mix 1 g bactoagar in 50 mL ddH₂O.

Heat slowly in microwave oven until the bactoagar has dissolved and a homogenous gel has formed. The gel must not be allowed to boil.

Keep warm in a water bath at 60 °C.

Keep at 4 °C between experiments.

65.2. Embedding of spheroids.

Day 1:

65.2.1. For each condition, Pool a minimum of 12 spheroids of each condition in a 1.5 mL Eppendorf tube (Figure 54A, (i)).

65.2.2. Wash once with 1 mL ice-cold PBS1 X PBS (Figure 5A, (ii)).

65.2.3. To fix the spheroids, add 1 mL of 4% paraformaldehyde.

65.2.4. Incubate for 24 h at room temperature (RT) (Figure 5A, (iii)).

Day 2:

65.2.5. Heat the agarose gel carefully by placing it in a water-filled beaker in a microwave in a water bath oven. The gel should not boil! Keep warm, e.g. in a benchtop heating plate, in water bath at 60 °C until use.

65.2.6. Wash spheroids twice with 1 mL ice-cold PBS1 X PBS (Figure 54A, (iv)).

65.2.7. Aspirate ~~approx. two thirds~~most of the PBS1 X PBS (leaving approximately 100 µl at this point is practical for handling the spheroids) (Figure 54A, (v)).

65.2.8. Prepare a 20 µL pipette by cutting the pipette tip at an incline to obtain a more pointy tip with a larger hole (see illustration).

Note: The next part has to be done quickly to ensure optimal spheroid transfer and to avoid solidification of gel drop. If no heating block is available, it is recommended to first catch the spheroids and then make the agarose drop (i.e. switching the order of points 65.2.9 and 65.2.10).

65.2.9. Make an agarose gel drop on a microscope slide (Figure 54A, (vi)). Place the slide on a warm heating block to prevent the agarose from solidifying.

65.2.10. Prepare a 20 µL pipette by cutting the pipette tip at an incline to obtain a more pointy tip with a larger hole (see illustration).

Using the modified pipette tip (see 65.2.8), ~~Catch~~ catch as many spheroids as possible in a volume of 15-20 µL.

~~— place the pipette on an object so the pipette is horizontal.~~

~~Make an agarose gel drop on an objective glass (Figure 4A, (vi)). If possible, place the objective glass on a warm heating block to prevent gel from solidifying. This will allow you to make the gel drop prior to catching spheroids, which will decrease the risk of spheroids sticking to the inside of the pipette.~~

65.2.11. Carefully inject the 15-20 µL spheroid-containing PBS1 X PBS into the center of the agarose gel drop without penetrating through the drop to the objective glass touching the microscope slide (Figure 54A, (vii)).

Note: This is a slightly difficult point. The spheroids will be lost if the pipette tip touches the microscope slide when injecting the spheroids into the gel drop. If the gel drop is accidentally penetrated when injecting the spheroids, they will be lost when the gel drop is pushed into the plastic tissue cassette. It is advisable to practice the whole process of making the agarose drop and injecting it injecting the spheroids, e.g. by injecting a colored liquid into the drop. This will allow visualization of a potential penetration through the drop, as the colored liquid will be leaking out of the gel drop onto the slide.

65.2.12. Let the agarose gel drop harden (5-10 min at RT or at 4 °C). Once the gel drop has solidified somewhat (it should still be pretty but still rather soft), carefully push the gel drop from the objective glass microscope slide into a plastic tissue cassette with a scalpel.

~~65.2.13. If the gel drop is accidentally penetrated when injecting the spheroids, there will be a liquid trace on the objective glass when the gel drop is pushed off.~~

~~Store~~Cover the plastic tissue cassettes in 70% ethanol.

Note: At this point the spheroids can be used directly or stored for months.

~~65.2.14. 11.~~ Embed the agarose-embedded spheroid in paraffin, section into 2-3 μm thick layer slides and stain with hematoxylin and eosin or subject to immunohistological staining.

~~6. Propidium iodide staining of spheroids~~

~~CAUTION: Propidium iodide (PI) should be handled in a fume hood and wearing gloves. PI is light sensitive. Protect from light when handling.~~

~~6.1. Make a PI solution of 4 μM by diluting stock solution in PBS.~~

~~This can be done by diluting a 1 mg/mL stock of PI in water 1:350 in PBS. This concentration will be further halved upon addition of the solution to the wells giving a final concentration of 2 μM . 100 μL of this solution is needed for each well containing a spheroid.~~

~~6.2. Go to the sterile cell culture lab and heat PBS to 37 $^{\circ}\text{C}$.~~

~~6.3. Remove 100 μL of the medium from each well in the 96-well plate without removing the spheroids.~~

~~6.4. Wash out the remaining medium by adding 100 μL of heated PBS to all wells followed by removing 100 μL of the liquid in the wells. Repeat this washing step 3 times.~~

~~6.5 Add 100 μL of the PI solution to each well, cover the plate in aluminum foil and place it in an incubator (37 $^{\circ}\text{C}$, 5% CO_2 , 95% humidity) for 10-15 min.~~

~~6.6. Repeat the 3 washing step described in step 4 to wash out PI solution, in order to diminish background signal when imaging.~~

~~6.7. Use an epifluorescence microscope to image the spheroids. To evaluate the viability of cells in the spheroid core take z-stacks to get images with varying depths of the spheroid.~~

~~A step size around 18-35 μm between each slice depending on spheroid size is advisable, giving approximately 11-18 stacks per spheroid.~~

~~Z-stacks can be processed in ImageJ using the z-projection function, which can combine all z-stacks into one final picture, giving an overview of the staining throughout the spheroid.~~

Representative results

Spheroid growth assays based on the spheroid formation protocol schematically illustrated in Figure 1A and B, were used as a starting point for analysis of effects of anti-cancer drug treatments in a 3D tumor mimicking setting. The ease with which spheroids are formed is cell line specific, and some cell lines require supplementation with rBM in order to form coherent spheroids²². The concentration of rBM added can profoundly affect the morphology of the spheroids. As shown in Figure 1C and D, varying the concentration of rBM ~~(in this case Geltrex)~~ between 0 and 4% alters the compactness and morphology of the spheroids in a cell type dependent manner. Figure 1C demonstrates how the addition of up to 2.5% rBM allows spheroid formation in SKBr-3 breast cancer cells, with no further effect at concentrations above 2.5% rBM. In contrast, BxPC3 pancreatic ductal adenocarcinoma (PDAC) cells, which exhibit an epithelial morphology, spontaneously form small, compact spheroids (Fig. 1D, upper, left panel). In this cell type, increasing rBM concentration to 1.5% or above elicits a distinct morphological change from spheroid to more convoluted structures with protrusions and invaginations, reminiscent of ductal tubular structure formation. Conversely, addition of rBM to two other PDAC cell lines, MiaPaCa and Panc-1, which have a more mesenchymal phenotype, allows the loose cellular aggregates to become tighter and form more compact spheroids (Figure 1D, middle and lower panels). These results show that the precise amount of rBM resulting in optimal spheroid formation must be titrated for each cell line and condition.

A quantitative assessment of cell viability within the spheroids upon drug treatment was necessary to evaluate the effect of anti-cancer drug treatments. The assay described here is a luciferin-luciferase-based assay, which measures ATP released from live cells within spheroids. An easily applicable assay for this purpose is the cell viability assay CellTiter-Glo 3D, the principle of the assay mechanism of which is illustrated in Figure 2A. ~~CellTiter-Glo 3D is a luciferin-luciferase-based assay, which measures ATP released from live cells within spheroids, giving rise to a~~ The luminescent signal generated in this assay is easily recorded by a plate reader (Figure 2A) and ~~which~~ correlates well with viability measured by other methods²³, ~~and which can be recorded by a plate reader (Figure 2A).~~ The linear relation between ATP concentration and luminescence in the relevant concentration range is shown in Figure 2B, while Figure 2C shows the ability of the assay to assess cell death in 3D spheroids treated with anti-cancer therapy. In order to further evaluate the linearity of the assay in the relevant range, experiments to establish standard curves of the luminescent signal as a function of the number of cells were carried out (Figure 2D and E). These results indicate that the assay is suitable for estimating cell viability in 3D spheroid cultures and that it is applicable for investigating drug-induced loss of cell viability.

A combination of light microscopic images acquired every two to three days during the treatment period and a final quantitative assessment of cell viability, allows close supervision of spheroid growth and morphology as well as assessment of optimal treatment dose. The latter is exemplified in Figure 3A and B, where a dose-response experiment was performed to determine the dose necessary for 50% reduced cell viability in MDA-MB-231 breast cancer spheroids. Treatment effects on spheroid morphology are visualized in Figure 3C and D for MDA-MB-231 and MCF-7 spheroids, respectively. During treatment with the chosen chemotherapeutic cocktail, the compactness of MDA-MB-231 spheroids increases, while during treatment with tamoxifen, MCF-7 spheroids become increasingly frayed and uneven. In both cases a clear drop in cell viability is visible after 7 (MDA-MB-231) or 9 (MCF-7) days of treatment (Figure 3E and F). This demonstrates the need for both a visual and a

quantitative assessment of treatment-mediated effects on spheroid cell viability and morphology as well as that these parameters are highly cell- and treatment-type specific.

As a supplement to the cell viability assay, staining of dead cells with PI, which cannot cross the membrane and therefore only stains necrotic or late apoptotic cells with compromised membrane integrity, allows for a quick spatial evaluation of dead cells in response to treatment, without the time-consuming protocol of embedding, sectioning and IHC. As illustrated in Figure 4A the spatial arrangement of dead cells upon an increasing concentration of an inhibitor, in this case the Na^+/H^+ exchanger 1 (NHE1) inhibitor 5-(N-ethyl-N-isopropyl)-amiloride (EIPA), can be visualized. As seen, control and vehicle spheroids show a limited necrotic/late apoptotic core, whereas the dead cells are distributed throughout the spheroid as the concentration of EIPA is increased.

In order to quantify the relative induction of apoptotic stress following different treatments, spheroids were lysed and subjected to SDS-PAGE gel electrophoresis and western blotting for full-length and cleaved poly (ADP-ribose) polymerase (PARP). Representative results are shown in Figure 4B and -C. In this experiment, spheroids were prepared from MDA-MB-231 cells in which the lactate-proton cotransporter MCT4 or the $\text{Na}^+/\text{HCO}_3^-$ cotransporter NBCn1, or both proteins in combination, were knocked down using siRNA. The knockdown was evaluated by western blotting for MCT4 and NBCn1 (not shown). As seen, the knockdown of MCT4, but not of NBCn1, robustly increases PARP cleavage, consistent with our previous demonstration that stable knockdown of MCT4 in MDA-MB-231 cells decreases tumor growth *in vivo* ²⁴.

To further analyze the effects of treatment and obtain information on, e.g., the specific signaling-, growth arrest, and death pathways activated, the spheroids can *in addition* to be either lysed and subjected to western blot analysis be, or embedded and subjected to immunohistochemistry (IHC) analysis. IHC analysis of the spheroid sections allows the use of specific antibodies or markers of, e.g. cell proliferation, cell cycle and programmed cell death, and facilitates a visualization of the spatial arrangement of e.g. proliferative and apoptotic cells in the spheroid.

AA schematic figure of the embedding protocol for IHC analysis of spheroids and a representative image of an $\approx 3\ \mu\text{m}$ thick microtome section of an embedded spheroid are presented in Figure 4A-5A. A representative light microscopic image of an approx. $\approx 3\ \mu\text{m}$ thick microtome section of an embedded spheroid and is shown in Figure 5B, and an immunofluorescence image of a spheroid stained for the tumor suppressor protein p53 (nuclei stained using DAPI), respectively is shown as Figure 5C. IHC analysis of the spheroid sections allows the use of specific antibodies or markers of, e.g. cell proliferation, cell cycle and programmed cell death, and facilitates a visualization of the spatial arrangement of e.g. proliferative and apoptotic cells in the spheroid. Examples of DMSO and chemotherapy-treated spheroids stained for the cell proliferation marker the cell proliferation marker-Ki-67 and/or for the tumor suppressor protein-p53 are shown in Figure 4C-5D and 5E, respectively. As expected Consistent with the antiproliferative effect of the chemotherapy treatment, the number of Ki-67 positive cells is greater in the DMSO-treated control spheroid, compared to than in the chemotherapy-exposed-treated spheroid (Figure 5D). In contrast, when staining against p53 expression is increased, which is indicative of during conditions of cell stress, apoptosis and growth arrest, and consequently, the number of p53-stained cells is substantially higher in the chemotherapy-treated spheroids compared to DMSO controls (Figure 5E).

~~As a supplement to the cell viability assay, staining of dead cells with PI, which cannot cross the membrane and therefore only stains necrotic or late apoptotic cells with compromised membrane integrity, allows for a quick spatial evaluation of dead cells in response to treatment, without the time consuming protocol of embedding, sectioning and IHC. As illustrated in Figure 4E the spatial arrangement of dead cells upon an increasing concentration of an inhibitor, in this case the NHE1 inhibitor 5 (N ethyl N isopropyl) amiloride (EIPA), can be visualized. As seen, control and vehicle spheroids show a limited necrotic/late apoptotic core, whereas the dead cells are distributed throughout the spheroid as the concentration of EIPA is increased.~~

These results ~~demonstrate~~ illustrate examples of two methods ~~show~~ for obtaining spatially resolved (PI staining, IHC) or quantitative (western blotting) information on drug treatment effects in 3D spheroids can be obtained.

Figure legends:

Figure 1. Spontaneous and rBM-mediated spheroid formation. protocols and examples. (A) Schematic representation of spheroid formation using ultra-low attachment ~~(ULA)~~ 96-well round bottom plates, with optional use of rBM. Individual steps marked by (i-iii). (B) Schematic representation of spheroid formation using the hanging drop method. Individual steps are marked by (i-iii) (C) Representative images of rBM-mediated spheroid formation of SKBr-3 cells. Cells were seeded in ultra-low attachment ULA 96-well round bottom plates with increasing concentrations of rBM ~~in the form of LDEV free, reduced growth factor Geltrex rBM~~, and grown for 9 days. Scale bar: 100 μ m. 3 n. (D) Representative images of BxPC-3, MiaPaCa and Panc-1 cells seeded for spheroid formation in ultra-low attachment ULA 96-well round bottom plates with concentrations of rBM from 0.5-2.5 %. Spheroids were grown for 4 days. Scale bar: 250 μ m. 3 n.

Figure 2. Principle and evaluation of the cell viability assay. (A) Schematic representation of the 3D cell viability assay, ~~CellTiter Glo 3D~~. Individual steps denoted by (i-iv). (B) Luminescent signal as a function of ATP concentration. Dilutions of ATP were plated in a 96-well plate and CellTiter-cell viability reagent added to each well. Luminescence was recorded after 30 min at 405 nm. 1 n. (C) Viability, measured as luminescence, of control and chemotherapy-treated MCF-7 spheroids. MCF-7 cells were seeded in ultra-low attachment ULA round-bottom plates, and were grown for 7 days. Chemotherapy treatment (5 μ M Cisplatin, 5 μ M Doxorubicin and 30 nM 5-FU) was applied on day 2 and 4. Bars represent mean values with SD. 1 n. (D) Luminescent signal as function of the number of MCF-7 cells s seeded. MCF-7 cells were seeded in 96-well plates at the indicated cell number and allowed to grow for 48 hours, after which cell viability was measured. Error bars represent SD. 1 n. (E) As described in D for MDA-MB-231 cells.

Figure 3. Effects of treatment regimens on spheroid morphology and cell viability. (A) Representative images of MDA-MB-231 spheroids on day 2, 4 and 7. MDA-MB-231 cells were seeded in ULA-ultra-low attachment -round bottom 96-well plates. ~~Treatment with, grown 7 days and treated with~~ increasing doses of chemotherapy was started on day 2 ~~and 4, at which time all spheroids were of similar size.~~ Rows show spheroids at increasing doses of chemotherapy, and columns show spheroids representative of size at day 2, 4, and 7 at the indicated dose. The lowest dose was 18.75 nM Cisplatin, 18.75 nM Doxorubicin, 0.0625 nM

5-Fluorouracil (5-FU), and this dose was doubled for each image shown, resulting in a maximal dose of 0.3 μ M Cisplatin, 0.3 μ M Doxorubicin and 2 nM 5-FU. Scale bar: 100 μ m. 2 n. (B) Viability of MDA-MB-231 spheroids, measured as luminescence, after 7 days of chemotherapeutic treatment. The bars represent mean values with SEM. 2 n. (C₁+D) Representative images of MDA-MB-231 (C) and MCF-7 spheroids (D) on day 2, 4, 7 and for MCF-7 spheroids 9. Cells seeded as in (A) and treated with either chemotherapy (Chemo, 18.75 nM Cisplatin, 18.75 nM Doxorubicin, 0.0625 nM 5-FU) on day 2 and 4 (C) or with 2 μ M Tamoxifen (Tam) on day 2, 4 and 7 (D). Scale bar: 100 μ m. 4 n and 3 n, respectively. (E₁+F) Viability, measured as luminescence, on day 7 and 9 for (C) and (D), respectively. To test for statistically significant difference between conditions an unpaired Student's t-test was performed. **** denotes $p < 0.0001$.

Figure 4. Propidium iodide staining and western blot analysis of spheroids. (EA) Representative images of PI-stained MCF-7 spheroids after 9 days of treatment. MCF-7 cells were seeded as described in Figure 3A, in ultra-low attachment 96-well plates grown for 9 days and treated with increasing concentrations of EIPA on day 2, 4 and 7. On day 9, the spheroids were stained with PI and images were acquired on an epifluorescence microscope. Scale bar: 200 μ m. 1 n.

(B) Representative western blots of MDA-MB-231 cells after knockout/knockdown of acid-base transporters NHE1 KO spheroids. Na⁺/H⁺ exchanger 1 (NHE1) was knocked out by CRISPR/Cas9 in MDA-MB-231-NHE1 KO cells¹² and the cells were subsequently transiently transfected with siRNA against MCT4, or NBCn1, or both and grown as spheroids for 9 days before being lysed and subjected to western blotting with using an antibody recognizing total and cleaved (c)PARP-antibodies. (C) Quantification of the relative ratio of cPARP to PARP protein level, normalized to loading control (β -actin). 1 n.

B-Xxx Western blots

Figure 45. Fixing, embedding and immunohistochemistry analysis of spheroids. (A) Schematic representation of the protocol for embedding of spheroids. Individual steps are marked as (i-vii). (B) Image of embedded MDA-MB-231 spheroid. Scale bar: 50 μ m. (C) Representative image of chemotherapy-treated MDA-MB-231 spheroid subjected to IHC analysis with antibodies against p-53. Dashed lines show the circumference of the spheroid. Scale bar: 20 μ m. (D₁+E)(C+D) Representative images of DMSO- or chemotherapy-treated (upper and lower panels, respectively) MDA-MB-231 spheroids. MDA-MB-231 cells were seeded in ultra-low attachment 96-well plates as described in Figure 3A, grown for 7 days and treated with chemotherapy on day 2 and 4. On day 7, the spheroids were embedded followed by analysis by IHC with primary antibodies against Ki-67 (DE) and p53 (EP). White boxes represent zoom images. Scale bar: 20 μ m in both magnifications. 3 n. (E) Representative images of PI-stained MCF-7 spheroids after 9 days of treatment. MCF-7 cells were seeded as described in Figure 3A, grown for 9 days and treated with increasing concentrations of EIPA on day 2, 4 and 7. On day 9, the spheroids were stained with PI and images were acquired on an epifluorescence microscope. Scale bar: 200 μ m. 1 n.

Discussion

The use of 3D cancer cell spheroids has proven a valuable and versatile tool not only for anticancer drug screening, but also for gaining mechanistic insight into the regulation of cancer cell death and viability under conditions mimicking those in the tumor microenvironment. This is particularly crucial as the accessibility, cellular uptake, and intracellular effects of chemotherapeutic drugs are profoundly impacted by the physico-chemical conditions in the tumor, including pH, oxygen tension, tortuosity, and physical and chemical cell-cell interactions^{9,17}. For example, the acidity of extracellular pH, which can reach values as low as 6-6.5 in many solid tumors²⁵⁻²⁹, causes weakly basic chemotherapeutic compounds, such as doxorubicin, mitoxantrone and the zwitterion paclitaxel, to be charged. This reduces their uptake into the tumor cells, and can influence the activity of multidrug resistance proteins such as p-glycoprotein³⁰⁻³². Also cell proliferation, which is pivotal to the effect of most chemotherapeutic compounds, is generally reduced in 3D compared to 2D conditions and hence is likely better mimicked in tumor spheroids than in 2D cell culture^{8,33,34}. Finally, the dense tumor microenvironment is the origin of numerous physical and soluble signaling cues directing intracellular signaling pathways regulating cell growth, survival and death. Thus, when analyzing drug efficacy, 3D culture systems are a pivotal step before embarking on *in vivo* models. A major drawback of 3D culture is, however, the increased complexity of analysis compared to that of 2D culture. We have described here simple and relatively inexpensive techniques for spheroid formation using a variety of cancer cell types. We have shown examples of how spheroid formation must be optimized for each cell type studied, and have described how to obtain quantitative data on cell viability, cell death, and associated signaling pathways, in such spheroids. There are no obvious growth- or morphological differences between the three models described here. In our hands, the variation in morphology may be slightly greater using the hanging drop method, yet an advantage of this method is that rBM is not needed. We have focused here on spheroids produced from a single cancer cell type. The spheroid model is, however, also amenable to co-culture, for instance of cancer cells with fibroblasts, monocytes/macrophages, endothelial cells, and/or adipocytes³⁵⁻³⁷. Other advanced applications of this model include the combination with 3D printed fluidic devices allowing dosing through a semipermeable membrane, followed by harvesting for quantitative proteomic profiling³⁸.

While, as noted above, the phenotype of cells grown in 3D spheroids generally mimics that of *in vivo* tumors much better than do cells grown in 2D, the extent to which such spheroids are in fact relevant models of the corresponding *in vivo* tumors is dependent on numerous factors, and has to be carefully evaluated. Parameters which will impact how well such spheroids mimic the *in vivo* condition include the cellular composition of the tumor and its relative ECM composition. For instance, the rBMmatrigel which we have employed as ECM in the protocols provided here is a good choice for mimicking early stages of epithelial cancers, around the time of breaching the basement membrane, other ECM compositions will be more relevant for certain tumor types and -stages. Furthermore, the capacity for cell-cell adhesion differs widely between cancer cell lines, depending on their expression of cell-cell and cell-matrix adhesion proteins such as cadherins and integrins²².

As described here, spheroid growth and morphology can easily and non-invasively be monitored every 2-3 days using a light microscope with low magnification optics and a large field of view. However, because cytotoxic stress such as chemotherapy treatment affects spheroid morphology very differently, and in a manner depending on the cell type and treatment scheme, ~~morphology and circumference are not~~ it is not sufficient to rely on morphology and circumference alone for evaluating treatment effect. For instance, spheroids

may become more loose with treatment and emerging cell death, or all death may occur in the necrotic core, while the surface is not detectably affected. In both cases, the result may be an erroneous impression that the number of live cells in the spheroid is not reduced by the treatment. Quantitative- and whole-spheroid techniques are therefore essential for evaluating treatment effect. For quantitative evaluation of cell death, the acid phosphatase assay, which as the name implies measures the activity of cytosolic acid phosphatase has been employed ²¹. However, in our hands, while this assay generally nicely reflects the number of cells seeded, it does not adequately capture rapid treatment-induced cell death (data not shown), likely because the acid phosphatase remains active for some time after cell death. Furthermore, this assay requires complete removal of the medium, which increases error especially with fragile, chemotherapy-treated spheroids. The cell viability assay described here, which is based on cellular ATP content, was chosen based on its simple and time efficient protocol and high reproducibility. Furthermore, this assay does not require complete removal of culture medium which is an advantage when working with spheroids. Other cell viability assays such as the acid phosphatase assay ²¹ can also be employed as long as they are adaptable to 3D cell cultures (see Discussion). As shown in Representative results, ~~we find that an assay based on the cellular ATP level~~this assay captures well both cell number and expected chemotherapy treatment effects. However, a pitfall of this technique is, obviously, that metabolic changes reducing intracellular ATP content may erroneously be recorded as a lower cell number. Hence, parallel assessment of, e.g. spheroid volume and morphology, or PI staining, is advisable to validate results.

Spheroid lysis followed by ~~w~~Western blotting can provide semi-quantitative insight into the state of signaling processes, cell death-, growth- and viability pathways. The use of ~~w~~Western blotting is complicated when rBMmatrigel is used to prepare the spheroids, since this will comprise a substantial fraction of the lysate protein content, and more importantly, its fractional contribution will increase with decreasing cellular content during chemotherapeutic cell death. It is in principle possible to remove the rBMmatrigel by centrifugation, however, ~~in our hands~~this is a critical step, as it is difficult to completely remove all rBM, and this will preclude quantitative comparison between conditions~~removal is rarely complete and results are compromised~~. For such spheroids, and in general for ~~qualitative, but~~ spatially resolved assessment of death pathways and relevant signaling parameters, embedding and IHC, ~~as shown in the Results section~~, are strong tools. Other approaches may be considered, e.g. live confocal imaging of (relatively small) intact spheroids ³⁹. Another interesting property of spheroids is that given their rather regular “ball” shape, they lend themselves well to iteration between mathematical modeling and wet lab experiments, to increase the understanding of the importance of, e.g., the above-mentioned gradients of oxygen, pH, and nutrients within spheroids, and, by extrapolation, tumors ^{40,41}. Thus, although important 3D tumor models of much greater complexity are emerging, including a wide range of organotypic and organoid cultures based on complex biological as well as inert scaffolds, and, not least, patient-derived xenografts ⁴², spheroids remain an important tool because of their superior biological relevance compared to 2D culture, combined with relative ease of handling.

In summary, we present here a series of simple methods for analysis of anti-cancer treatment-induced changes in cancer cell viability and death in 3D culture. The composition of the spheroids can be modified depending on the properties and biology of the cells employed, and the quantitative and qualitative analyses presented are useful both for

assessing dose-response relationships and for gaining insight into the signaling- and death pathways involved.

Disclosures

The authors declare no conflict of interest.

Acknowledgements

We are grateful to Katrine Franklin Mark and Annette Barteles for excellent technical assistance [and to Asbjørn Nøhr-Nielsen for performing the experiments in Figure 1D.](#)

This work was funded by the Ejnar Willumsen Foundation, the Novo Nordisk Foundation, and Fondation Juchum (all to SFP).

References

- 1 Sutherland, R. M. Cell and environment interactions in tumor microregions: the multicell spheroid model. *Science*. **240** (4849), 177-184, (1988).
- 2 Mueller-Klieser, W., Freyer, J. P. & Sutherland, R. M. Influence of glucose and oxygen supply conditions on the oxygenation of multicellular spheroids. *British Journal of Cancer*. **53** (3), 345-353, (1986).
- 3 Gaedtke, L., Thoenes, L., Culmsee, C., Mayer, B. & Wagner, E. Proteomic analysis reveals differences in protein expression in spheroid versus monolayer cultures of low-passage colon carcinoma cells. *Journal of Proteome Research* **6** (11), 4111-4118, (2007).
- 4 Chen, J. L. *et al.* The genomic analysis of lactic acidosis and acidosis response in human cancers. *PLoS Genetics* **4** (12), e1000293, (2008).
- 5 Cukierman, E., Pankov, R., Stevens, D. R. & Yamada, K. M. Taking cell-matrix adhesions to the third dimension. *Science*. **294** (5547), 1708-1712, (2001).
- 6 Gudjonsson, T., Ronnov-Jessen, L., Villadsen, R., Bissell, M. J. & Petersen, O. W. To create the correct microenvironment: three-dimensional heterotypic collagen assays for human breast epithelial morphogenesis and neoplasia. *Methods*. **30** (3), 247-255, (2003).
- 7 Pampaloni, F., Reynaud, E. G. & Stelzer, E. H. The third dimension bridges the gap between cell culture and live tissue. *Nature Reviews in Molecular and Cell Biology* **8** (10), 839-845, (2007).
- 8 Hirschhaeuser, F. *et al.* Multicellular tumor spheroids: an underestimated tool is catching up again. *Journal of Biotechnology* **148** (1), 3-15, (2010).
- 9 Jacobi, N. *et al.* Organotypic three-dimensional cancer cell cultures mirror drug responses in vivo: lessons learned from the inhibition of EGFR signaling. *Oncotarget*. **8** (64), 107423-107440, (2017).
- 10 Rodriguez-Enriquez, S. *et al.* Energy metabolism transition in multi-cellular human tumor spheroids. *Journal of Cell Physiology* **216** (1), 189-197, (2008).
- 11 Kunz-Schughart, L. A. Multicellular tumor spheroids: intermediates between monolayer culture and in vivo tumor. *Cell Biology International* **23** (3), 157-161, (1999).
- 12 Andersen, A. P. *et al.* Roles of acid-extruding ion transporters in regulation of breast cancer cell growth in a 3-dimensional microenvironment. *Molecular Cancer*. **15** (1), 45, (2016).

- 13 Swietach, P., Patiar, S., Supuran, C. T., Harris, A. L. & Vaughan-Jones, R. D. The role of carbonic anhydrase 9 in regulating extracellular and intracellular pH in three-dimensional tumor cell growths. *Journal of Biological Chemistry* **284** (30), 20299-20310, (2009).
- 14 Walenta, S., Doetsch, J., Mueller-Klieser, W. & Kunz-Schughart, L. A. Metabolic imaging in multicellular spheroids of oncogene-transfected fibroblasts. *Journal of Histochemistry and Cytochemistry* **48** (4), 509-522, (2000).
- 15 Kunz-Schughart, L. A., Groebe, K. & Mueller-Klieser, W. Three-dimensional cell culture induces novel proliferative and metabolic alterations associated with oncogenic transformation. *International Journal of Cancer*. **66** (4), 578-586, (1996).
- 16 Feng, H. *et al.* Homogeneous pancreatic cancer spheroids mimic growth pattern of circulating tumor cell clusters and macrometastases: displaying heterogeneity and crater-like structure on inner layer. *Journal of Cancer Research and Clinical Oncology* **143** (9), 1771-1786, (2017).
- 17 Santini, M. T., Rainaldi, G. & Indovina, P. L. Apoptosis, cell adhesion and the extracellular matrix in the three-dimensional growth of multicellular tumor spheroids. *Critical Reviews in Oncology/Hematology* **36** (2-3), 75-87, (2000).
- 18 Vinci, M. *et al.* Advances in establishment and analysis of three-dimensional tumor spheroid-based functional assays for target validation and drug evaluation. *BMC Biology* **10** 29, (2012).
- 19 Pickl, M. & Ries, C. H. Comparison of 3D and 2D tumor models reveals enhanced HER2 activation in 3D associated with an increased response to trastuzumab. *Oncogene*. **28** (3), 461-468, (2009).
- 20 Wong, C., Vosburgh, E., Levine, A. J., Cong, L. & Xu, E. Y. Human neuroendocrine tumor cell lines as a three-dimensional model for the study of human neuroendocrine tumor therapy. *Journal of Visual Experiments* 10.3791/4218 (66), e4218, (2012).
- 21 Friedrich, J. *et al.* A reliable tool to determine cell viability in complex 3-d culture: the acid phosphatase assay. *Journal of Biomolecular Screening* **12** (7), 925-937, (2007).
- 22 Ivascu, A. & Kubbies, M. Diversity of cell-mediated adhesions in breast cancer spheroids. *International Journal of Oncology* **31** (6), 1403-1413, (2007).
- 23 Crouch, S. P., Kozlowski, R., Slater, K. J. & Fletcher, J. The use of ATP bioluminescence as a measure of cell proliferation and cytotoxicity. *Journal of Immunological Methods*. **160** (1), 81-88, (1993).
- 24 Andersen, A. P. *et al.* The net acid extruders NHE1, NBCn1 and MCT4 promote mammary tumor growth through distinct but overlapping mechanisms. *International Journal of Cancer*. (2018).
- 25 Vaupel, P. Tumor microenvironmental physiology and its implications for radiation oncology. *Seminars in Radiation Oncology* **14** (3), 198-206, (2004).
- 26 Vaupel, P. W., Frinak, S. & Bicher, H. I. Heterogeneous oxygen partial pressure and pH distribution in C3H mouse mammary adenocarcinoma. *Cancer Research*. **41** (5), 2008-2013, (1981).
- 27 Helmlinger, G., Yuan, F., Dellian, M. & Jain, R. K. Interstitial pH and pO₂ gradients in solid tumors in vivo: high-resolution measurements reveal a lack of correlation. *Nature Medicine* **3** (2), 177-182, (1997).
- 28 Zhang, X., Lin, Y. & Gillies, R. J. Tumor pH and its measurement. *Journal of Nuclear Medicine* **51** (8), 1167-1170, (2010).

- 29 Gillies, R. J., Raghunand, N., Karczmar, G. S. & Bhujwalla, Z. M. MRI of the tumor microenvironment. *Journal of Magnetic Resonance Imaging*. **16** (4), 430-450, (2002).
- 30 Vukovic, V. & Tannock, I. F. Influence of low pH on cytotoxicity of paclitaxel, mitoxantrone and topotecan. *British Journal of Cancer*. **75** (8), 1167-1172, (1997).
- 31 Song, C. W., Griffin, R. & Park, H. J. in *Cancer Drug Resistance* (ed B. A. Teicher) 21-42 (Humana Press, 2006).
- 32 Lotz, C. *et al.* Role of the tumor microenvironment in the activity and expression of the p-glycoprotein in human colon carcinoma cells. *Oncology Reports* **17** (1), 239-244, (2007).
- 33 Sant, S. & Johnston, P. A. The production of 3D tumor spheroids for cancer drug discovery. *Drug Discovery Today: Technologies* **23** 27-36, (2017).
- 34 Stratmann, A. T. *et al.* Establishment of a human 3D lung cancer model based on a biological tissue matrix combined with a Boolean in silico model. *Molecular Oncology* **8** (2), 351-365, (2014).
- 35 Kuen, J., Darowski, D., Kluge, T. & Majety, M. Pancreatic cancer cell/fibroblast co-culture induces M2 like macrophages that influence therapeutic response in a 3D model. *PLoS One*. **12** (7), e0182039, (2017).
- 36 Bochet, L. *et al.* Adipocyte-derived fibroblasts promote tumor progression and contribute to the desmoplastic reaction in breast cancer. *Cancer Research* **73** (18), 5657-5668, (2013).
- 37 Amann, A. *et al.* Development of a 3D angiogenesis model to study tumour - endothelial cell interactions and the effects of anti-angiogenic drugs. *Scientific Reports* **7** (1), 2963, (2017).
- 38 LaBonia, G. J., Ludwig, K. R., Mousseau, C. B. & Hummon, A. B. iTRAQ Quantitative Proteomic Profiling and MALDI-MSI of Colon Cancer Spheroids Treated with Combination Chemotherapies in a 3D Printed Fluidic Device. *Analytical Chemistry* **90** (2), 1423-1430, (2018).
- 39 Hulikova, A., Vaughan-Jones, R. D. & Swietach, P. Dual role of CO₂/HCO₃⁻ formula buffer in the regulation of intracellular pH of three-dimensional tumor growths. *Journal of Biological Chemistry* **286** (16), 13815-13826, (2011).
- 40 Wallace, D. I. & Guo, X. Properties of tumor spheroid growth exhibited by simple mathematical models. *Frontiers in Oncology* **3** 51, (2013).
- 41 Michel, T. *et al.* Mathematical modeling of the proliferation gradient in multicellular tumor spheroids. *Journal of Theoretical Biology* **458** 133-147, (2018).
- 42 Meijer, T. G., Naipal, K. A., Jager, A. & van Gent, D. C. Ex vivo tumor culture systems for functional drug testing and therapy response prediction. *Future Science OA*. **3** (2), FSO190, (2017).